Isotopic records of terrestrial ice age environments in mammoth bioapatite

Laura Arppe

Academic dissertation

To be presented,
with the permission of the Faculty of Science of the University of Helsinki,
for public criticism in lecture room E204 of Physicum, Kumpula, on
November 20th, 2009, at 12 o'clock noon.

Publications of the Department of Geology D17
Helsinki 2009

Ph.D. thesis No. 204 of the Department of Geology, University of Helsinki

Supervised by:
Professor Juha Karhu
Department of Geology
University of Helsinki
Finland

Reviewed by:
Dr. Kathryn A. Hoppe
University of Washington
USA

and

Dr. Thomas Tütken
Universität Bonn
Germany

Discussed with:
Professor Hervé Bocherens
Universität Tübingen
Germany

Cover: Mammoth molar in gravel (photo: J.Karhu)

ISSN 1795-3499
ISBN 978-952-10-4275-1 (paperback)
ISBN 978-952-10-4276-8 (PDF)
http://ethesis.helsinki.fi/

Helsinki 2009
Yliopistopaino

Laura Arppe: Isotopic records of terrestrial ice age environments in mammoth bioapatite, University of Helsinki, 2009, 52pp., University of Helsinki, Publications of the Department of Geology D17, ISSN 1795-3499, ISBN 978-952-10-4275-1, ISBN 978-952-10-4276-8 (pdf-version).

Abstract

Palaeoenvironments of the latter half of the Weichselian ice age and the transition to the Holocene, from ca. 52 to 4 ka, were investigated using isotopic analysis of oxygen, carbon and strontium in mammal skeletal apatite. The study material consisted predominantly of subfossil bones and teeth of the woolly mammoth (*Mammuthus primigenius* Blumenbach), collected from Europe and Wrangel Island, northeastern Siberia. All samples have been radiocarbon dated, and their ages range from >52 ka to 4 ka. Altogether, 100 specimens were sampled for the isotopic work.

In Europe, the studies focused on the glacial palaeoclimate and habitat palaeoecology. To minimise the influence of possible diagenetic effects, the palaeoclimatological and –ecological reconstructions were based on the enamel samples only.

The results of the oxygen isotope analysis of mammoth enamel phosphate from Finland and adjacent nortwestern Russia, Estonia, Latvia, Lithuania, Poland, Denmark and Sweden provide the first estimate of $\delta^{18}O$ values in glacial precipitation in northern Europe. The glacial precipitation $\delta^{18}O$ values range from ca. -9.2±1.5‰ in western Denmark to -15.3‰ in Kirillov, northwestern Russia. These values are 0.6-4.1‰ lower than those in present-day precipitation, with the largest changes recorded in the currently marine-influenced southern Sweden and the Baltic region. The new enamel-derived $\delta^{18}O$ data from this study, combined with oxygen isotope records from earlier investigations on mammoth tooth enamel and palaeogroundwaters, facilitate a reconstruction of the spatial patterns of the $\delta^{18}O$ values of precipitation and palaeotemperatures over much of Europe. The reconstructed geographic pattern of $\delta^{18}O$ in precipitation during 52-24 ka reflects the progressive isotopic depletion of air masses moving northeast, consistent with a westerly source of moisture for the entire region, and a circulation pattern similar to that of the present-day. The application of regionally varied δ/T-slopes, estimated from palaeogroundwater data and modern spatial correlations, yield reasonable estimates of glacial surface temperatures in Europe and imply 2-9°C lower long-term mean annual surface temperatures during the glacial period.

The isotopic composition of carbon in the enamel samples indicates a pure C3 diet for the European mammoths, in agreement with previous investigations of mammoth ecology. A faint geographical gradient in the $\delta^{13}C$ values of enamel is discernible, with more negative values in the northeast. The spatial trend is consistent with the climatic implications of the enamel $\delta^{18}O$ data, but may also suggest regional differences in habitat openness.

The palaeogeographical changes caused by the eustatic rise of global sea level at the end of the Weichselian ice age was investigated on Wrangel Island, using the $^{87}Sr/^{86}Sr$

ratios in the skeletal apatite of the local mammoth fauna. The diagenetic evaluations suggest good preservation of the original Sr isotope ratios, even in the bone specimens included in the study material. To estimate present-day environmental ^{87}Sr/^{86}Sr values on Wrangel Island, bioapatite samples from modern reindeer and muskoxen, as well as surface waters from rivers and ice wedges were analysed. A significant shift towards more radiogenic bioapatite Sr isotope ratios, from 0.71218 ± 0.00103 to 0.71491 ± 0.00138, marks the beginning of the Holocene. This implies a change in the migration patterns of the mammals, ultimately reflecting the inundation of the mainland connection and isolation of the population. The bioapatite Sr isotope data supports published coastline reconstructions placing the time of separation from the mainland to ca. 10-10.5 ka ago. The shift towards more radiogenic Sr isotope values in mid-Holocene subfossil remains after 8 ka ago reflects the rapid rise of the sea level from 10 to 8 ka, resulting in a considerable reduction of the accessible range area on the early Wrangel Island.

Contents

List of publications

The thesis is based on the following original publications, referred to by the Roman numerals (I-IV), as well as some previously unpublished data by the author.

I **Arppe, L.M.**, Karhu, J.A., 2006. Implications for the Late Pleistocene climate in Finland and adjacent areas from the isotopic composition of mammoth skeletal remains. Palaeogeography, Palaeoclimatology, Palaeoecology 231, 322-330.

II Ukkonen, P., **Arppe, L.**, Kjær, K., Houmark-Nielsen, M., Karhu, J.A., 2007. MIS 3 mammoth remains from Sweden – implications for faunal history, palaeoclimate and glaciation chronology. Quaternary Science Reviews 26, 3081-3098.

III **Arppe, L.**, Karhu, J.A., Vartanyan, S.L., 2009. Bioapatite $^{87}Sr/^{86}Sr$ of the last woolly mammoths – implications for the isolation of Wrangel Island. Geology 37, 347-350.

IV **Arppe, L.**, Karhu, J.A. Oxygen isotope values of precipitation and the thermal climate in Europe during the middle to late Weichselian ice age. Submitted to Quaternary Science Reviews.

The author's contribution to the publications

The author planned and performed the sampling, and conducted the isotopic and chemical analyses in all four papers.

I The study was planned by J. Karhu. The data was interpreted and the article written jointly by both authors.

II The study was planned by P. Ukkonen, and the isotopic part by L. Arppe. P. Ukkonen, K. Kjær and M. Houmark-Nielsen were responsible for the osteological part, faunal and glacial history, and sedimentological interpretations. L. Arppe and J. Karhu were responsible for the isotope part: L. Arppe interpreted the data together with J. Karhu, and had the main responsibility for writing the isotope-related parts of the article.

III The study was planned by J. Karhu, who together with S. Vartanyan also collected the sample material, and provided background information relevant to the study site and the material. L. Arppe interpreted the data with J. Karhu, and prepared the manuscript to be edited by the other authors.

IV The study is based on an idea developed by L. Arppe and J. Karhu. It was planned, conducted and written by L. Arppe. J. Karhu took part in the interpretation of the results, organisation and editing of the manuscript.

1 Introduction

The Weichselian ice age (ca. 115-11 ka), its termination and the transition to the Holocene warm period signified major changes in past global environments. Compared to the present-day conditions, the glacial palaeoenvironments were characterised with a different composition and distribution of fauna and flora (e.g. van Andel and Tzedakis, 1996; Huntley et al., 2003; Lister and Stuart, 2008). Changing orbital parameters induced significant insolation changes (e.g. van Meerbeeck et al., 2009). Glacial surface temperatures were generally lower than at present, and the climate was markedly unstable, with frequent fluctuations between cold stadial and warmer interstadial intervals (e.g. Johnsen et al., 1992; Voelker et al., 1998). The presence of ice sheets on the Eurasian and American continents and the effect of the expanded ice masses on the global sea level caused changes in topography and the distribution of land and sea (e.g. Peltier, 1994; Lambeck et al., 2002). In addition to significantly lowered levels, the glacial seas experienced temperature and circulation changes (e.g. Broecker et al., 1990).

Most of these palaeoenvironmental changes are known from high resolution ice core and marine records (Johnsen et al., 1992; Grootes et al., 1993; Fairbanks, 1989; Voelker et al., 1998). In contrast, terrestrial records of the ice age environments on the continents, especially those of quantitative nature, are fragmentary at best (Voelker et al., 2002). They are particularly poor in the regions covered by the continental ice-sheets at their late maximum extent, eradicating the environmental archives of the antecedent glacial time period. In these areas, the palaeoenvironmental record contained in mammal skeletal remains can prove invaluable.

Fossil skeletal remains are a source of a wealth of information on the environments of the past. The composition of animal assemblages (e.g. Stuart and Lister, 2001), and the physiological parameters of the skeletal parts themselves allow for interpretations of the palaeoenvironment (e.g. Fortelius et al., 2002). The use of the isotopic tracers in skeletal apatite was introduced to the scientific community in the early 1980's. The carbon isotope composition of animals was found to contain ecological information reflecting the consumed diet (DeNiro and Epstein, 1978; Land et al., 1980; Sullivan and Krueger, 1981), and the Sr isotope composition in mammal skeletons was recognised as a potential tracer of migration and residence (Gosz et al., 1983; Ericson, 1985). Oxygen isotope ratios of mammal bones were proven useful in palaeohydrological and –climatological work (Longinelli, 1984; Luz et al., 1984a).

This work focuses on the insights into the glacial environments afforded by the isotopic ratios of oxygen, carbon and strontium in mammal skeletal apatite. Skeletal remains of the woolly mammoth (*Mammuthus primigenius* Blumenbach) were recognised as promising material for the isotopic reconstructions because of their abundance in the glacial fossil record, their large size, and often well constrained ages through ^{14}C dating. Three lines of investigation were followed, each based on different isotopes. Two separate geographical areas were chosen as locations for the application of the isotope studies.

The glacial palaeoclimate of Europe was investigated using the oxygen isotope composition in mammoth bioapatite. The isotopic ratios of carbon in the bioapatite were used to gain information on the characteristics of the animals' habitat in Europe via the consumed diet. The effect of sea level change to the local palaeogeography was studied on Wrangel Island, northeastern Siberia, using the Sr isotope composition of the local mammoth fauna.

1.1 Skeletal apatite

Calcified tissues of vertebrate skeletons consist of a mineral component, organic material and water. The inorganic phase is composed almost entirely of calcium phosphates, more precisely a form of carbonate hydroxyapatite. The generalised chemical formula for skeletal calcium phosphates can be given as $Ca_{10}(PO_4)_6X_2$, with X denoting a variety of ions, the most frequent being hydroxyl (OH^-), fluoride (F^-), and carbonate (CO_3^{2-}) (Hillson, 2005). Considering the most common substitutions, an approximate chemical composition for primary skeletal apatite is $Ca_{8.86}Mg_{0.09}Na_{0.29}K_{0.01}[(HPO_4)_{0.28}(CO_3)_{0.41}](PO_4)_{5.31}]$ x $[OH_{0.70}Cl_{0.08}(CO_3)_{0.05}]$ (Elliott, 2002).

The different skeletal tissues most commonly used in palaeoenvironmental research – bone, dental enamel and dentine – display significant dissimilarities on many scores. Bone is a porous material, with a very small crystal size of hydroxyapatite and a high content of organic matter (~30% of dry weight), mostly in the form of collagen. Bone remodels throughout life: bone tissue is continuously removed and new tissue is generated (Elliott, 2002).

In contrast, tooth enamel is essentially non-porous. It is almost entirely inorganic, containing ca. 96% bioapatite, less than 1% organic material, and water (Williams and Elliott, 1989). The size of the hydroxyapatite crystals is an order of magnitude larger than that in bone (Hillson, 2005). Amelogenesis, the formation of dental enamel, takes place in two stages: matrix production and maturation. During maturation, the organic matter and water, which in the original matrix amount to two thirds by weight, are removed and the apatite crystals increase in size to produce a dense, highly mineralised enamel tissue (Hillson, 2005). Compared to tooth enamel, dentine is more porous, and has a much smaller crystal size and lower inorganic content (Driessens and Verbeeck, 1990; Williams and Elliott, 1989; Hillson, 2005).

Unlike bone, dentine and enamel form by accretion, and are not remodeled after the initial crystallisation (Hillson, 2005). Thus, the environmental indicators recorded by dental tissues during tooth growth often represent conditions of a relatively short time period, with emphasis on the early phases of the animal's life.

Mammoth teeth, which represent the overwhelming majority of the study material in this thesis, are continually formed along the animal's lifespan. Mammoths have six sets of molariform teeth erupting in sequence through life, with one or two teeth per dentition quadrant in wear at a time. As a tooth is slowly worn out, it moves forward in the jaw, and a replacement tooth erupts from behind. The third permanent molar is the last to erupt and wear, thus marking the natural limit to a mammoth's life (Hillson, 2005; Haynes, 1991).

1.2 Isotopic compositions of skeletal apatite

1.2.1 Definitions

The isotopic compositions of oxygen and carbon are reported as δ values, defined as the permil (‰) difference from the international reference standards VSMOW (Vienna Standard Mean Ocean Water) for oxygen, and VPDB (Vienna Peedee Belemnite) for carbon. In the δ-notation,

$$\delta = (R_{sample}/R_{standard} - 1) \times 1000,$$

R is the isotopic ratio, $^{18}O/^{16}O$ or $^{13}C/^{12}C$, and δ is $\delta^{18}O$ or $\delta^{13}C$. The isotopic composition of strontium is given as the $^{87}Sr/^{86}Sr$ ratio.

1.2.2 $^{18}O/^{16}O$

The skeletal parts of mammals form at a constant temperature of ~37 °C. Therefore, the oxygen isotope composition of the precipitating skeletal apatite is determined solely by the isotopic composition of the animal's body water (Longinelli, 1984; Luz et al., 1984a). In large mammals, the $\delta^{18}O$ value of body water is mainly dependent on that of ingested environmental waters (Bryant and Froelich, 1995), which usually corresponds to the mean $\delta^{18}O$ value in regional precipitation ($\delta^{18}O_{ppt}$).

Most of the global precipitation is derived from evaporation occurring in the tropical latitudes. As the air masses move along temperature gradients from tropical to polar latitudes, inland from the sea, and to higher elevations, condensation controlled mainly by adiabatic cooling preferentially removes water with the heavier isotopes, ^{18}O and ^{2}H, from the vapour. The process can be described by a Rayleigh model (Craig, 1961; Dansgaard, 1964), and results in the characteristic geographic pattern of $\delta^{18}O$ levels in global precipitation with isotope compositions progressively more depleted in ^{18}O and ^{2}H in higher latitudes and altitudes (Rozanski et al., 1993; Bowen and Wilkinson, 2002). The $\delta^{18}O_{ppt}$ values in the middle and high latitudes are linearly correlated to the mean annual surface temperature at the precipitation site (Dansgaard, 1964; Rozanski et al., 1982; 1992; 1993). The relationship equals to 0.69 ‰ $°C^{-1}$ for high northern latitude coastal stations (Dansgaard, 1964), and 0.59‰ $°C^{-1}$ in continental Europe (Rozanski et al., 1992).

The link between the $\delta^{18}O$ values of mammal bioapatite ($\delta^{18}O_{ap}$) and ingested meteoric waters ($\delta^{18}O_{w}$), and the strong relationship between temperature and the $\delta^{18}O_{ppt}$ value provide a basis for using $\delta^{18}O$ values recovered from mammal skeletal remains in palaeoclimatological research. For palaeoclimatological work, the oxygen bound to the phosphate component is often preferred due to diagenesis-related reasons (see below), but also the oxygen present in the structural carbonate is often used. To convert the $\delta^{18}O_{ap}$ levels measured in fossil skeletal apatite to oxygen isotope values of the meteoric waters, the relationship between $\delta^{18}O_{ap}$ and $\delta^{18}O_{w}$ has to be quantified. $\delta^{18}O_{ap}$- $\delta^{18}O_{w}$ fractionations calibrated on analogous extant animals are often applied in oxygen isotope studies of fossil taxa, as the parameters of the equations are usually scaled according to the physiology of the animal (e.g. Bryant and Froelich, 1995; Kohn, 1996). For mammoths, an equation calibrated on modern elephants, thought to have a similar body size and comparable feeding habits to those of the mammoths (Ayliffe et al., 1992; Ukraintseva, 1986), has been shown applicable (Ayliffe et al., 1992; Ayliffe et al., 1994; Genoni et al., 1998; Jones et al., 2001; Tütken et al., 2007; 2008).

The climatic information contained in mammal bioapatite $\delta^{18}O$ values has been used to derive estimates of regional mean values and temporal variations of $\delta^{18}O$ in past precipitation from recent times back to millions of years ago (e.g. Bryant et al., 1994, 1996a; Fricke et al., 1995; Genoni et al., 1998; Koch et al., 1998; Hoppe, 1999; Iacumin et al., 2004; Bentaleb et al., 2006; Tütken et al., 2006; 2007).

1.2.3 $^{13}C/^{12}C$

The $\delta^{13}C$ value of the carbonate fraction in herbivore skeletal apatite reflects the $\delta^{13}C$ of the ingested plants, which in turn is dependent on the mechanism of photosynthesis. Virtually all trees, most shrubs, herbs and cool-climate grasses and sedges follow the C3 photosynthetic pathway, also called the Calvin cycle, and display $\delta^{13}C$ values from -35 to -22‰, with a mean at -27‰ (e.g. O'Leary, 1988; Cerling et al., 1999). Plants using the C4 pathway, i.e. Hatch-Slack cycle, are mostly tropical grasses and some sedges. They display less negative $\delta^{13}C$ values, from -15 to -10‰, averaging -13‰. A third group of plants, arid-climate succulents, employ a mechanism called crassulacean acid metabolism (CAM), which combines features of both C3 and C4 pathways and results in intermediate plant $\delta^{13}C$ values.

Bioapatite $\delta^{13}C$ values of large herbivores are offset from the plant isotope values by about 14‰ (Cerling and Harris, 1999). Thus, animals consuming modern C3 vegetation can display bioapatite $\delta^{13}C$ levels from -20 to -8‰, with mean values around -13 to -12‰. Correspondingly, C4 feeders usually show bioapatite $\delta^{13}C$ values from 0 to +5‰ (Kohn and Cerling, 2002). During the glacial period, plant carbon isotope compositions were more positive than today due to changes in the concentration and the isotopic composition of atmospheric CO_2 (e.g. Marino and McElroy, 1991; Marino et al., 1992), thus resulting in correspondingly shifted $\delta^{13}C$ values in herbivores (e.g. Koch et al., 1998). According to Marino et al. (1992), the $\delta^{13}C$ value of the atmospheric CO_2 was ca. 1‰ higher during lateglacial times (14-10 ^{14}C kyr BP), and ca. 0.5 ‰ higher in the full glacial (> 20 ^{14}C kyr BP).

Because of the links between animal $\delta^{13}C$ values, diet and environment, the analysis of the carbon isotope ratios in bioapatite has been applied in a variety of palaeodietary, –ecological and environmental investigations (e.g. Lee-Thorp et al., 1989; Quade et al., 1992; Cerling et al., 1993, 1999; Bocherens et al., 1994; Gadbury et al., 2000; Iacumin et al., 2000; Feranec, 2004; Hoppe and Koch, 2006; Drucker et al., 2008).

1.2.4 $^{87}Sr/^{86}Sr$

Sr substitutes Ca in the skeletal carbonate hydroxyapatite. As the bioapatite accepts virtually no rubidium, new ^{87}Sr is not produced by the decay of ^{87}Rb and the $^{87}Sr/^{86}Sr$ ratio of the precipitated biomineral can be considered stable. Due to the small relative mass difference between strontium isotopes, the $^{87}Sr/^{86}Sr$ ratio is not affected by measurable fractionation during weathering or incorporation into the skeletal apatite.

The $^{87}Sr/^{86}Sr$ ratio of herbivore skeletal apatite is equal to that of the consumed plants, which in turn tracks the isotopic composition of biologically available Sr in the soil of foraging areas (e.g. Sillen et al., 1998). The isotopic composition of Sr in soils is affected mainly by local geological units and atmospheric input (Gosz et al., 1983; Graustein and Armstrong, 1983; Graustein, 1989; Miller et al., 1993; Chadwick et al., 1999). On average, $^{87}Sr/^{86}Sr$ of animal skeletal apatite reflects regional trends of Sr isotope values in local geological formations (e.g. van der Merwe et al., 1990; Vogel et al., 1990; Hoppe et al., 1999).

The $^{87}Sr/^{86}Sr$ value of a geological unit depends on its initial $^{87}Sr/^{86}Sr$ ratio, the Rb content and its age. Very old rock units with high Rb concentrations, such as Precambrian low-Ca granitic rocks, will have high $^{87}Sr/^{86}Sr$ ratios, whereas young volcanics are placed in the lower end of the Sr ratio scale. Phanerozoic marine limestones reflect the relatively low Sr isotope levels of the ocean from which they were precipitated (~0.7069 to 0.7092; McArthur et al., 2001). Sedimentary rocks can display a wide range of Sr isotopic values depending upon the source of the mineral material.

Rather than directly repeating the average $^{87}Sr/^{86}Sr$ value of the underlying bedrock, soil solutions often display a range of Sr ratios determined by the degree of geological heterogeneity, differential weathering of minerals, and mixing of sediment from various provenances (e.g. Sillen et al., 1998; Price et al., 2002). Despite the sometimes high variability in local environmental Sr isotope ratios, the $^{87}Sr/^{86}Sr$ values in the bioapatite of local animals have been reported to exhibit surprising intra-population consistency (Price et al., 2002).

As the $^{87}Sr/^{86}Sr$ ratio of herbivore skeletal apatite is ultimately derived from the bedrock, fossil bioapatite can be used as an indicator of past feeding areas (Gosz et al., 1983**;** Sealy et al., 1991; Sillen et al., 1998). The approach has been used in a number of archaeological investigations (e.g. Müller et al., 2003; Price and Gestsdóttir, 2006) and in reconstructing the migratory behavior of, e.g., fish (Koch et al., 1992), birds (Chamberlain et al., 1997), and mammoths and mastodons (Hoppe et al., 1999; Hoppe 2004; Hoppe and Koch 2006; 2007).

1.3 Diagenetic effects

After deposition, the original, biogenic isotopic compositions in the skeletal apatite are subject to alteration in diagenetic processes (e.g. Nelson et al., 1986; Ayliffe et al., 1994; Lee-Thorp and Sponheimer, 2003; Tütken et al., 2008). These include, e.g., dissolution and reprecipitation of apatite, precipitation of secondary minerals, as well as chemical and isotopic exchange between the bioapatite and the diagenetic fluids. In order to reliably reconstruct environmental conditions at the time of biomineralisation, the recognition of post-mortem alteration is essential. Significant differences in the propensity to isotopic alteration among different skeletal apatite tissues, chemical components within the bioapatite and elements have been observed.

The dissimilarities in the retention of original isotope signatures between skeletal tissues arise from differences in organic content, porosity and crystallinity. Due to its attributes, bone mineral is highly susceptible to dissolution and reprecipitation of secondary mineral phases, often resulting in the loss of the original isotopic compositions (e.g. Ayliffe et al., 1994; Hoppe et al., 2003; Lee-Thorp and Sponheimer, 2003). In contrast, tooth enamel is considered to be most resistant to post-depositional alteration and hence is the preferred skeletal tissue for isotopic investigations (Nelson et al., 1986; Lee-Thorp and van der Merwe, 1991; Ayliffe et al., 1994; Bryant et al., 1994; 1996b; Koch et al., 1997; Budd et al., 2000; Sharp et al., 2000; Price et al., 2002; Hoppe et al., 2003; Lee-Thorp and Sponheimer, 2003; Zazzo et al., 2004a).

The chemical components within skeletal apatite show differential propensities for alteration of the oxygen isotope composition. The $\delta^{18}O$ values of the structural carbonate component ($\delta^{18}O_c$) are more readily altered (Shemesh et al., 1983; Nelson et al., 1986; Iacumin et al., 1996a), and experiments by Zazzo et al. (2004a) imply that the standard acetic acid pretreatments are not necessarily able to restore pristine carbonate isotope compositions. The oxygen isotope values of the phosphate fraction ($\delta^{18}O_p$) of the biogenic apatite have the potential to remain stable in inorganic conditions over very long time periods (Kolodny et al., 1983; Luz et al., 1984b; Lécuyer et al., 1999; Kohn et al., 1999) due to exceptional strength of the P–O bonds (Tudge, 1960). However, significant alteration of the isotope ratios of PO_4 is possible during microbially mediated reactions (Blake et al., 1997; Zazzo et al., 2004a; 2004b), even in enamel.

The effects of diagenesis on the carbon isotope values of bioapatite follow the general pattern of superior preservation in enamel compared to other skeletal tissues (Quade et al., 1992; Wang and Cerling, 1994; Koch et al., 1997; Lee-Thorp, 2000). Some investigations have deemed bone and dentine $\delta^{13}C$ values irreversibly altered (e.g. Schoeninger and deNiro, 1982; Koch et al., 1997), while some suggest that also bone can retain original isotopic compositions (e.g. Lee-Thorp, 2000).

Original biogenic Sr concentrations and isotopic compositions in fossil skeletal tissues are readily obscured due to post-mortem contamination by strontium from the burial environment. The porous and less crystalline tissues, bone and dentine, are especially susceptible to diagenetic Sr imprinting (e.g. Nelson et al., 1986; Sillen, 1986; Budd et al., 2000; Hoppe et al., 2003), and the use of enamel as sample material for Sr isotope work is strongly recommended (e.g. Budd et al., 2000; Price et al., 2002; Hoppe et al., 2003).

1.4 Aims of the study

This work is aimed at recovering the signals recorded in the isotope compositions of mammoth skeletal remains reflecting the palaeoenvironment during the later half of the Weichselian ice age and the large-scale changes that occurred with the transition to the present interglacial. The study sought answers to questions in three general research areas – climatic patterns and palaeotemperatures, habitat palaeoecology, as well as sea level change and palaeogeography.

More specifically, the thesis endeavours

1) to determine the $\delta^{18}O$ values of glacial precipitation in central areas affected by the Scandinavian Ice Sheet in northern Europe on the basis of the oxygen isotope ratios in mammoth bioapatite from Finland, northwestern Russia, Sweden, Denmark, Estonia, Latvia, Lithuania and Poland;
2) to present a synthesis of the spatial and temporal variations of $\delta^{18}O_{ppt}$ over much of Europe during MIS 3 and early MIS 2 at 52-24 ka, thus shedding light on the pattern of atmospheric circulation, moisture transport and the process of isotopic distillation of water vapour during the glacial period over Europe; and
3) to describe the European glacial climate through the reconstruction of palaeotemperatures;
4) to investigate if spatial and/or temporal variability can be detected in the diet of the European mammoths and, thus, their habitat; and finally,
5) to determine the timing and progress of the isolation process of Wrangel Island in northeastern Siberia.

Together these aims form answers to the broader research question, “How are the circumstances of the Weichselian ice age and its termination manifested in the stable isotope records of mammoth bioapatite?”

2 Material and methods

2.1 Mammoth skeletal remains

The sample material consists almost entirely of skeletal remains of the woolly mammoth, which was common across Eurasia during the Weichselian ice age (Stuart et al., 2002).

For the palaeoenvironmental studies in Europe, altogether 49 specimens of mammoth bones (n=2) and teeth (n=47) from Finland and adjacent northwestern Russia, Sweden, Denmark, Estonia, Latvia, Lithuania and Poland were sampled (Fig. 1; Table 1 in Papers I and IV; Table 7 in Paper II). Of the tooth specimens, 44 were molars, from which tooth enamel was sampled, and 3 were tusks. The mammoth remains have been discovered from different sedimentological contexts. Nearly all specimens are geological stray finds, transported and reworked into their find localities by the Scandinavian Ice Sheet (SIS). Observations from Finland (Ukkonen et al., 1999), Denmark (Aaris-Sørensen, 2006) and Sweden (Paper II) indicate that glacial transport distances have been relatively short, from a few kilometers to a few tens of kilometers, and the finds therefore are thought to represent local or regional fauna. The mammoth remains from Poland have been discovered from the Middle

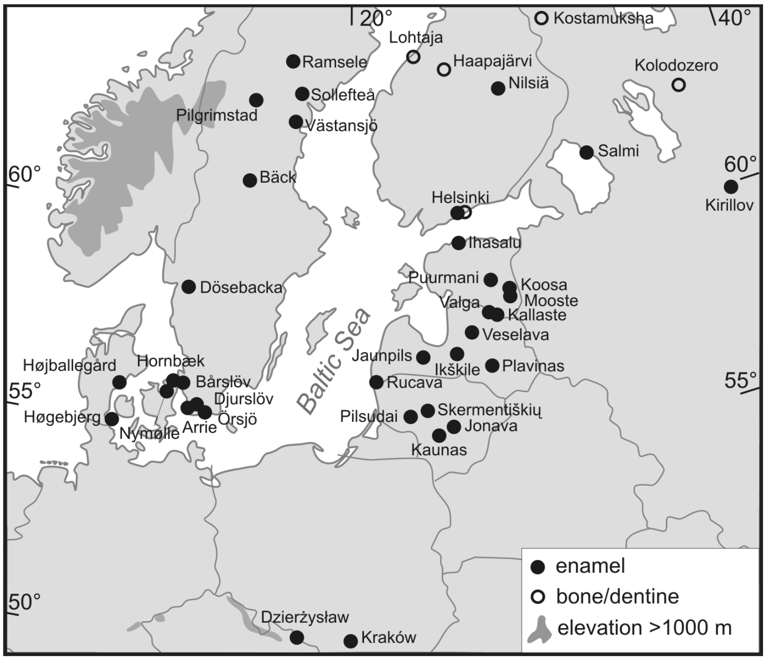

Figure 1. Locations of the analysed European mammoth finds.

and Upper Palaeolithic archaeological sites of Spadzista Street (B, C, E and F) and Zwierzyniec on the St. Bronisława hill in Kraków, and Dzierżysław near Kraków, and represent material found nearly *in situ* (Wojtal and Sobczyk, 2005). Detailed documentations of the sampled specimens are provided by Aaris-Sørensen et al. (1990) and Aaris-Sørensen (2006) for Denmark, Lõugas et al. (2002) for Estonia, Ukkonen et al. (1999) for Finland, and Paper II for Sweden.

The site of the palaeogeographical $^{87}Sr/^{86}Sr$ study, Wrangel Island, is situated in the Arctic Ocean, between the East Siberian Sea and the Chukchi Sea, 140 km north of the Chukotka peninsula coast (Fig. 2). For the study, 51 specimens of mammoth (n=40), muskox (*Ovibos moschatus*) (n=6), reindeer (*Rangifer tarandus*) (n=3) and bison (*Bison priscus*) (n=2) teeth and bones were sampled (Supplementary Table DR1 in Paper III). The material consists primarily of tooth enamel (n=41), but also bones (n=10) were sampled to improve the temporal coverage of the data. The skeletal parts were collected from river banks (Krasny Flag, Neizvestnaya and Tundrovaya rivers on the northern coastal plain, Gussinaya river in the west, and Neozhidannya and Mamontovaya rivers in the southwest), coastal beaches and from slope and alluvial fan deposits.

2.2 Chronological control

Dates for the European specimens were either derived from literature, or they were dated in conjunction with the study. Radiocarbon dates for the Finnish and Estonian specimens were taken from Ukkonen et al. (1999) and Lõugas et al. (2002), respectively. The dates for the specimens from Nymølle, Denmark, and Bårslöv, Sweden, were obtained from Aaris-Sørensen (2006). The other specimens from Sweden (Paper II) and Denmark (Paper IV), as well as those from Latvia, Lithuania and Poland (Paper IV) were ^{14}C (AMS) dated at the GeoBiosphere Science Centre Radiocarbon Dating Laboratory, Lund University, Sweden. For conversion of the primary radiocarbon data into calendar ages, various protocols and programs were used. Paper I employs the coral data of Bard (1998) (Table I in Paper I). The ^{14}C dates of the molar specimens used for the isotopic work in Paper

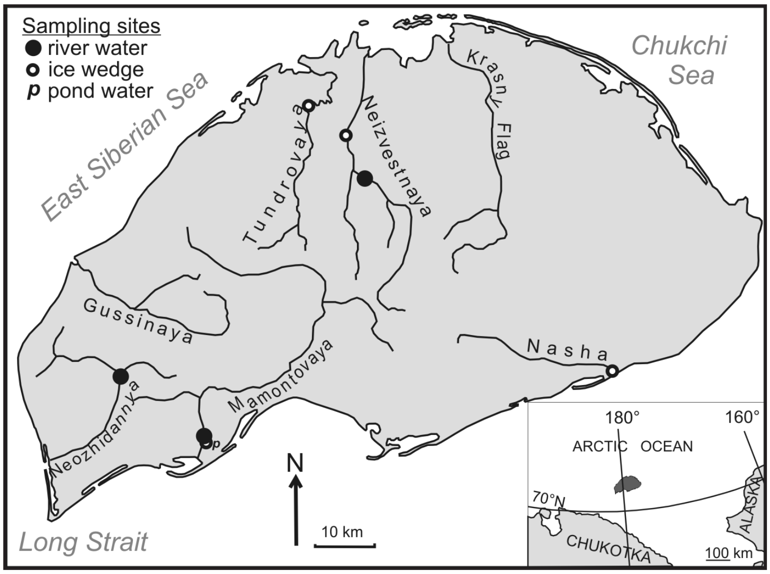

Figure 2. Map of Wrangel Island showing the major rivers where the mammoth specimens were collected, and the surface water sampling localities. Modified from Paper III.

II were calibrated using the calibration curves recommended by the NotCal04 members, compiled in van der Plicht et al. (2004) (Table 7 in Paper II). In Paper IV, the CalPal-2007 program (Weninger et al., 2008) and the Hulu age model (Weninger and Jöris, 2008) was used to convert conventional ^{14}C ages into the calendric time scale (Table 1 in Paper IV).

The use of different calibration curves and programs can lead to over 1000-year discrepancies in the resulting calendar ages (Weninger et al., 2007). In order to facilitate combination of the enamel $\delta^{18}O$ and $\delta^{13}C$ data, the primary finite ^{14}C dates from Finland, adjacent northwestern Russia (Paper I) and Sweden (Paper II), as well as all cited mammoth bioapatite dates from other studies, were recalibrated using CalPal/Hulu (Weninger et al., 2008; Weninger and Jöris, 2008). These calendar ages, given in the Appendix and Table 1 of Paper IV, are used in the following discussions of the European mammoth enamel $\delta^{18}O$ and $\delta^{13}C$ data.

All the specimens for the $^{87}Sr/^{86}Sr$ study on Wrangel Island have been radiocarbon dated in previous studies. The majority of the skeletal remains on Wrangel Island have Holocene ages. Out of 124 ^{14}C determinations, only 18 date from beyond 11 ka (Vartanyan et al., 2008). No mammoth finds have been reported from the time interval 14-10 ka. The primary dates, derived from Vartanyan et al. (2008), were converted to calendar years by using the online version of Calib 5.0.2 (Stuiver et al., 2005) and the IntCal04 data (ages <21 000 ^{14}C yr BP; Reimer et al., 2004), and the Fairbanks0107 calibration curve based on Fairbanks et al. (2005) (ages > 21 000 ^{14}C yr BP). The age of the remains spans the time period from >52 ka to recent.

2.3 Monitoring of isotopic alteration

The oxygen isotope fractionation between $\delta^{18}O_p$ and $\delta^{18}O_c$ of skeletal apatite was used to check if the primary oxygen isotope values had been preserved (e.g. Iacumin et al., 1996a; 1996b; Genoni et al., 1998). In addition, to assess the degree of diagenetic chemical alteration (Kohn et al., 1999), the concentrations of selected elements were determined on the mammoth specimens from Finland and adjacent Russia (Paper I).

To check for preservation of biogenic $^{87}Sr/^{86}Sr$ ratios, untreated sample aliquots from two specimens were analysed alongside aliquots pretreated with acetic acid applying different reaction times (Paper III).

2.4 Isotopic and chemical analyses

With a few exceptions, the analyses of the isotopic composition of carbon, phosphate oxygen and carbonate oxygen were performed on aliquots of the same sample. The samples were taken either by a diamond-tip drill (Paper I) or by detaching fragments from the enamel lamellae (Papers II and IV) after first removing the outermost surface of the bone or tooth. Typically, sampled fragments measured 1.5-2 cm in the direction of enamel growth increments, representing ≥ 1 year of growth (see Hoppe and Koch, 2006).

For the analysis of the isotopic composition of oxygen in phosphate, the silver phosphate method was applied following the chemical procedures of O´Neil et al. (1994) and Stephan (2000) with some modifications. To remove organic contaminants, the samples were treated with 3% NaOCl + NaOH solution for 24 h and rinsed with deionised water. The procedure was performed twice for bone and dentine samples. The pretreated sample powder was dissolved in 1 M HNO_3. Calcium and other interfering ions were removed by cation exchange chromatography. The phosphate ion was precipitated as Ag_3PO_4. The precipitate was reduced under vacuum by graphite at 1340°C and the resulting CO_2 was used for isotope determinations. The oxygen isotope ratios were measured on a Finnigan MAT 251 dual inlet gas mass spectrometer at the Geological Survey of Finland, Espoo (GTK). The external precision of a $\delta^{18}O_p$ measurement determined from multiple sample measurements was better than 0.3‰. Measurements of the NIST phosphate rock standard NBS-120b gave a value of 22.5 ± 0.4‰ (n=18). The equation of Ayliffe et al. (1992) calibrated with modern elephants (excluding data from arid regions) was used to correlate the $\delta^{18}O_p$ values measured from mammoth enamel with the $\delta^{18}O_w$ values of ingested meteoric waters.

The oxygen and carbon isotope compositions of the structural carbonate were analysed at GTK (Papers I and II) and at the Department of Geology, University of Helsinki (Paper IV). The pretreatment procedure followed that of Bocherens et al. (1996a). At GTK, the analysis followed the principles of the sealed vessel phosphoric acid method by McCrea (1950), with a 1 h reaction time at 100°C. The isotope ratios of oxygen and carbon of the cryogenically purified CO_2 were measured on a Finnigan MAT 251 dual inlet mass spectrometer. The external precision based on multiple sample measurements was better than 0.1‰ for $\delta^{13}C$, 0.2‰ for $\delta^{18}O_c$. The phosphoric acid fractionation factor of Swart et al. (1991) for calcite was used to correct for the effects of the acid reaction in the analysis of the carbonate fraction (but see Passey et al., 2007). At the Department of Geology, University of Helsinki, the samples were analysed at 70 °C using a ThermoFinnigan Gasbench II coupled to a ThermoFinnigan Delta^{Plus} Advantage continuous flow mass spectrometer (Paper IV; Spötl and Vennemann, 2003). The measured oxygen and carbon isotope data were normalised to an in-house calcite standard calibrated against the calcite standard NBS-19. Duplicate analyses (n=14) of sample aliquots indicate a reproducibility of ±0.05‰ for $\delta^{13}C$ and ±0.1‰ for $\delta^{18}O_c$. The carbon and oxygen isotope values are expressed in the δ-notation as permil (‰), relative to the VPDB and VSMOW standards, respectively.

For the samples from Finland and adjacent northwestern Russia the contents Al, Ba, Cu, Fe, Mn, Si and Sr were determined using ICP-AES, and the distribution of Fe and Mn in the enamel samples was investigated using a scanning electron microprobe (Paper I).

The skeletal apatite samples for the analysis of $^{87}Sr/^{86}Sr$ were pretreated by soaking the powders in 0.1N acetic acid (CH_3COOH) for 10 minutes, washing them with distilled and deionised water, and repeating the procedure. Pretreated samples were first dissolved in 4N HNO_3 and evaporated to dryness. Organic residues in some of the bone samples were removed with additions of concentrated

HNO_3 and evaporation to dryness. The dry samples were then dissolved in 1N HNO_3. Strontium was extracted on microcolumns using Eichrom Sr-spec resin, and the Sr-containing solution was evaporated to dryness. Sr samples dissolved in 0.75N H_3PO_4 were loaded on Ta-filaments for measurement. $^{87}Sr/^{86}Sr$ ratios were measured on a VG Sector 54 mass spectrometer at GTK. Sr isotope ratios were corrected for instrumental mass fractionation using the ratio of $^{86}Sr/^{88}Sr = 0.1194$. As a measure of precision and accuracy of the analytical procedure, the SRM 987 strontium standard gave a value of 0.710250 ± 0.000023 (1 SD, n = 8). The internal precision of single measurements was better than ± 0.00004 (2SE). In addition to samples of skeletal apatite, water samples from surface waters and ice wedges on Wrangel Island were analysed to gain information on the range of local present-day environmental Sr isotope compositions. The waters were filtered with a 0.45 µm filter, evaporated to dryness, and then taken up with 1N HNO_3 for Sr extraction. The analysis and measurement procedures followed those described for the bioapatite samples.

3 Results and Discussion

3.1 Radiocarbon dating

Radiocarbon dating is important for studies based on mammal skeletal remains. The normal confidence limits of radiocarbon dating and calibration for dates ≥ 20 000 ^{14}C yr BP, and differences between various calibration (Weninger and Jöris, 2008; Fairbanks et al., 2005) and comparison (van der Plicht et al., 2004) schemes provide a time frame in the scale of ± hundreds–few thousand years for the mammoth data. This is sufficient for the detection of longer-term trends, but pinpointing ^{14}C dated mammoth specimens to specific short-term events, such as the millennial scale Dansgaard-Oeschger fluctuations, is not feasible within these age uncertainties.

There are no significant differences in the calendar ages given by the recommended IntCal04 dataset and programs (Reimer et al., 2004), and the CalPal/Hulu calibration in the age range 0 to 11 kyr ^{14}C BP (Weninger et al., 2007). For the lateglacial radiocarbon ages 14-12 ^{14}C kyr BP the CalPal/Hulu calibration results in calendric ages up to 600 yrs older than IntCal04 due to the inclusion of the Cariaco-Hulu dataset (Hughen et al., 2006) in the CalPal/Hulu curve construction. However, these discrepancies would not change the assignment of the specimens to specific lateglacial warm/cold stages.

The differences of the available calibration procedures are reflected in the outcome of the first calibrations (Papers I and II) and recalibrations (Paper IV) of the pre-LGM specimens from Finland, adjacent northwestern Russia, and Sweden. The recalibration by CalPal/Hulu gives mean calendar ages for the molars with finite dates in Paper I up to 670 years older compared to Bard (1998). However, the original calendar dates are within the 95% range given in Paper IV. The CalPal/Hulu recalibration of the Swedish specimens results in 2000-6000 years narrower age ranges. The large spread of calendar age estimates produced by the NotCal04 comparison curves (van der Plicht et al., 2004) is mostly due to a significantly different shape of the Bahama speleothem (Beck et al., 2001) and Lake Suigetsu (Kitagawa and van der Plicht, 1998; 2000) curves, not included in the CalPal/Hulu calibration.

The Fairbanks0107 calibration (Fairbanks et al., 2005) used for the > 21 ^{14}C kyr BP Wrangel samples, and the CalPal/Hulu calibration generally yield mean calendar ages within the 1σ range, but differences in mean ages can reach 1000 years in > 30 ^{14}C kyr BP samples. Thus, the calendar ages of the Wrangel Island specimens are not fully comparable to those from Europe.

3.2 Preservation and significance of the primary isotopic signatures

3.2.1 Oxygen and carbon isotopes

Assessing the effects of diagenesis on the different mammoth skeletal tissues from Finland and adjacent northwestern Russia was a major focus of Paper I. The results of the chemical analyses suggest 10-1000 –fold increases in the concentrations of most analysed elements in some of the bone and dentine specimens relative to those in modern African herbivore enamel (Paper I; Kohn et al., 1999). These changes are most likely due to diagenetic precipitation of secondary Fe-Mn-Ba –bearing oxides, oxyhydroxides and the presence of clay minerals (Elorza et al., 1999; Kohn et al., 1999) in the pore spaces and microscopic fractures within apatite. Increases in the concentrations of Fe, Mn, Al and Si can be detected also in the enamel samples, although not as dramatic as those observed in the bone specimens. SEM-spot analyses indicate that the elevated concentrations in enamel most likely represent a mixed analysis of unaltered, pristine apatite with no measurable Fe or Mn, and dark Fe-Mn –rich coatings, present on the diagonal growth surfaces and cracks of the lamellae (Paper I).

While the determined elemental concentrations do not provide information on the possible isotopic alteration of the species of interest, they suggest that all samples bear signs of diagenetic changes. It should be noted, that the baseline values taken to represent modern, unaltered levels may not be a suitable point of comparison for the mammoth samples, as suggested by the investigation of Sponheimer and Lee-Thorp (2006) stressing the need for geologically appropriate modern/fossil comparisons. Regardless, the variance observed in the elemental concentrations of the mammoth bioapatite samples can provide information on the relative strength of diagenetic effects, which seem to be most dramatic in the bone specimens (Paper I).

The reliability of the oxygen isotope signal was evaluated by comparing the $\delta^{18}O_c$ and $\delta^{18}O_p$ values. The phosphate and structural carbonate fractions of the hydroxyapatite precipitate under the same equilibrium conditions with the body fluid, producing a systematic offset between $\delta^{18}O_p$ and $\delta^{18}O_c$ ($\Delta^{18}O_{C-P}$), which averages ~9‰ for mammals (Bryant et al., 1996b; Iacumin et al., 1996a). Checking for the preservation of this characteristic isotopic spacing, or comparing the $\delta^{18}O_p$ and $\delta^{18}O_c$ values to the fractionation line representing equilibrium ($\delta^{18}O_P = 0.98 \times \delta^{18}O_C - 8.5$; Iacumin et al., 1996a) represent valid tests of isotopic fidelity in biogenic samples (e.g. Martin et al., 2008; Zazzo et al., 2004b; 2009).

The enamel samples form a tight group close to the equilibrium fractionation line (Fig. 3), consistent with well preserved original oxygen isotope values. Further, one dentine and one bone specimen appear to be in oxygen isotope equilibrium, although the elemental concentrations of Fe, Mn and Ba in these samples imply the strongest diagenetic effects relative to the other specimens (Paper I). Three specimens, representing two dentine and one bone sample lie further apart and show $\Delta^{18}O_{C-P}$ offsets ≤ 6.2‰, suggesting isotopic disequilibrium. Judging from their position relative to the expected fractionation (Fig. 3), either the oxygen isotope composition of phosphate has shifted to more positive values, or that of the carbonate component has decreased as a result of diagenetic alteration, or both components have changed. While

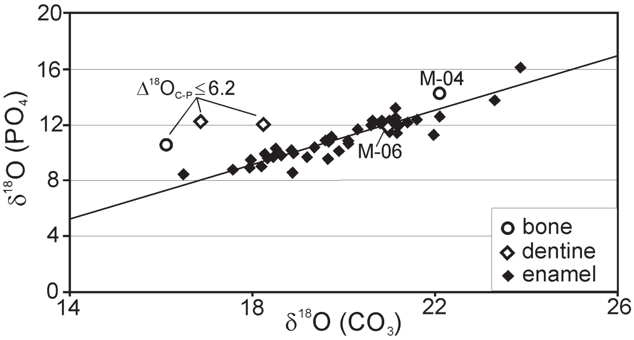

Figure 3. The relationship of $\delta 1^{8}O_{PO4}$ and $\delta^{18}O_{CO3}$ in the European mammoth bioapatite specimens. The line ($\delta^{18}O_{PO4} = 0.98 \times \delta^{18}O_{CO3} - 8.5$) represents isotopic equilibrium according to Iacumin et al. (1996a).

structural carbonate is generally considered more susceptible to post-depositional alteration (Land et al., 1980; Nelson et al., 1986; Iacumin et al., 1996a), and as such the likely candidate responsible for the disequilibrium, diagenetic changes in the phosphate fraction are also possible. Raised $\delta^{18}O_p$ values can result from, e.g., reprecipitation of phosphate in equilibrium with local groundwaters in Finland (Paper I) or by isotopic exchange in microbially mediated reactions (Blake et al., 1997; Zazzo et al., 2004a; 2004b). Bone material is particularly susceptible to the latter mechanism, whereas enamel is affected to a lesser extent (Zazzo et al., 2004a).

The preservation of the $\delta^{13}C$ values cannot be tested in a similar manner as the $\delta^{18}O$ values, because the mineral part of bioapatite holds only one pool of carbon, i.e. the structural carbonate component. However, a comparison of the bioapatite $\delta^{13}C$ values to those determined from collagen in the same specimens (Table 1 in Paper I) provides a means to estimate diagenetic alteration of the bioapatite carbon isotope ratios (e.g. Land et al., 1980). The carbon isotope fractionation between collagen and the mineral component of skeletal apatite should be ~8‰ (Sullivan & Krueger, 1981), and for natural diets it may vary between 7–10‰ (e.g. Lee Thorp et al., 1989; Bocherens and Mariotti, 1992). Except for one dentine sample, all specimens display $\delta^{13}C_{collagen} - \delta^{13}C_{carbonate}$ offsets in the expected range, and the $\delta^{13}C$ values of both components are similar to those reported by Iacumin et al. (2000) and Bocherens et al. (1996b) for Eurasian mammoths. The dentine sample M-06 shows a 19.1‰ difference between the $\delta^{13}C$ values of collagen and structural carbonate, suggesting isotopic alteration (Paper I).

Based on the diagenetic assessments of the samples from Finland and adjacent northwestern Russia, and the findings of prior studies on differential alteration of skeletal tissues discussed earlier, only the enamel samples were considered for the palaeoenvironmental reconstructions (Paper I). Accordingly, only enamel was sampled for the isotopic reconstructions in the studies presented in Papers II and IV. Similarly to the enamel samples reported in Paper I, those from Sweden, Denmark, the Baltic countries, and Poland display $\Delta^{18}O_{C\text{-}P}$ offsets consistent with the biogenic fractionation (Papers II and IV). Plotted on a $\delta^{18}O_c$–$\delta^{18}O_p$ diagram, their analysis points cluster near the equilibrium fractionation line (Fig. 3). No collagen $\delta^{13}C$ data were available for these samples, so direct testing for carbon isotope alteration was not possible. However, it can be argued that if the oxygen isotope ratio in the carbonate component is unaltered, then there is a good chance that also carbon has preserved its original isotope value (e.g. Land et al., 1980; Zazzo et al., 2009). Furthermore, the $\delta^{13}C$ values of the specimens from Sweden, Denmark, the Baltic countries and Poland are all within the range of unaltered $\delta^{13}C_{carbonate}$ values reported in Paper I and, thus, are likely to have retained their original compositions.

The $\delta^{18}O_w$ values calculated from $\delta^{18}O_p$ may not be representative of local precipitation if the ingested waters have been significantly affected by evaporation, causing ^{18}O enrichment, or by inclusion of ^{18}O-depleted glacial melt waters. Prior studies of ice age climates (Ayliffe et al., 1992; Genoni et al., 1998; Fox et al., 2007; Tütken et al., 2007) indicate that evaporation has not affected the glacial ingestion waters of the mammoths to the extent that the $\delta^{18}O_p$-$\delta^{18}O_w$ correlation (Ayliffe et al., 1992) would fail to produce reasonable estimates of $\delta^{18}O_{ppt}$. (Ayliffe et al., 1992; Genoni et al., 1998; Fox et al., 2007; Tütken et al., 2007). The effect of glacier melt waters, however, is a relevant concern, though there is no evidence of melt waters biasing $\delta^{18}O_w$ values reconstructed from mammoth bioapatites in Europe (Ayliffe et al., 1992; Genoni et al., 1998; Tütken et al., 2007; 2008). No glaciers exist, nor were likely to have existed during Marine Isotope Stage 3 (MIS 3 ≈ 59-29 ka) in the vicinity of the study areas in Finland, the Baltic countries and Poland. Furthermore, the small extent of the SIS during that period, restricted to the Scandinavian mountains (Arnold et al., 2002), suggests that even the mammoths of Sweden and Denmark lived tens to hundreds of kilometers from the ice sheet margin and its melt water. Therefore, negligible influence of ^{18}O –depleted glacial melt water is assumed, and the calculated $\delta^{18}O_w$ values are taken to closely represent $\delta^{18}O$ values of precipitation.

The isotopic composition of the enamel samples reflects averaged environmental conditions of the area where the animal ranged during the formation of the enamel. Ruling out hypotheses of transcontinental migrations in the order of ~2000 km (Churcher, 1980), more recent isotope studies in North America indicate that mammoths did not regularly undertake migrations of more than a few hundred kilometres and may have ranged only locally (Hoppe et al., 1999; Hoppe, 2004). Woolly mammoths of eastern Europe are thought to have migrated according to seasonal food availability analogously to modern elephants moving over distances of 200-300 km (Velichko and Zelikson, 2005). Thus, it is reasonable to assume that the isotopic records in the mammoth bioapatite reflect the average environmental conditions on a regional scale, within a few hundred kilometers from the site of discovery.

3.2.2 Strontium isotopes

Diagenetic strontium is usually associated with secondary pore-filling mineral phases, which have different solubilities than the original bioapatite (Sillen, 1986). Various pretreatment procedures have been applied to separate biogenic Sr from secondary Sr derived from the depositional environment. Most procedures employ leaching with a weak acid solution, but differ in reaction time, amount of acid per sample and acid strength (e.g. Sillen, 1986; Hoppe et al., 1999; Budd et al., 2000; Hoppe et al., 2003; Sponheimer and Lee-Thorp, 2006). Whereas the acetic acid pretreatment effectively removes diagenetic contaminants from enamel (Budd et al., 2000; Hoppe et al., 2003; Sponheimer and Lee-Thorp, 2006), retrieving a reliable biogenic signal from bone samples has been proven difficult (Budd et al., 2000; Hoppe et al., 2003). However, exceptions are known: in some cases even enamel has been irreversibly altered (Koch et al., 1992), while there is also evidence of bone retaining primary Sr isotope signatures (Sillen et al., 1998). The variability in the retention of original Sr signatures highlights the significance of taphonomic history and the depositional environment to the differential physical, chemical and isotopic preservation of skeletal remains (Lee-Thorp and Sponheimer, 2003; Sponheimer and Lee-Thorp, 2006).

Wrangel Island has an extremely cold and dry arctic climate. The mean annual temperature and amount of precipitation are -11.3°C and ~200 mm, respectively, and the terrain is in permafrost. The conditions are ideal for the preservation of fossil remains, as testified by the preservation of soft tissues, hair and food in the intestine of mammoth carcasses discovered from Siberia (e.g. Dima and the Berezovka mammoth; Herz, 1902; Shilo et al., 1983, both cited by Haynes, 1991). The results of the pretreatment experiments suggest a minimal to nonexistent presence of diagenetic Sr in the enamel samples, and thus their $^{87}Sr/^{86}Sr$ ratios can be viewed as the primary, *in vivo* signatures (Paper III). Meanwhile, Hoppe et al. (2003) reported all untreated samples, including tooth enamel, to yield Sr isotope ratios different from expected biogenic values. The contrasting findings presented in Paper III probably reflect significant differences in the depositional environment.

The effectiveness of the pretreatment was not tested on bone samples, and there, the influence of secondary Sr cannot be entirely ruled out. However, based on the range of $^{87}Sr/^{86}Sr$ ratios displayed by the surface water samples from the island, post-depositional alteration in the local diagenetic environment would tend to increase the Sr isotope ratios in Pleistocene bones. The majority of the old bone samples, including all >45 ka bones, have retained a Sr signature distinct (lower) from that of the diagenetic environment, and no trend in bone $^{87}Sr/^{86}Sr$ to higher values with increasing sample age can be detected. These observations imply that no pervasive diagenetic imprinting has occurred in the bone samples, and support the view that also their $^{87}Sr/^{86}Sr$ ratios represent biogenic signatures.

3.3 European palaeoenvironment during MIS 3 to 2

The maximum late Weichselian ice cover (LGM) in the western Baltic Sea region was reached at ca. 22-20 ka (Wysota et al., 2002; Houmark-Nielsen, 2004), and ca. 21-19 ka in the southeastern parts (Rinterknecht et al., 2006). The mammoth enamel dates cover a time period from >50 ka to 11 ka (Appendix and Table 1 in Paper IV). The majority of the specimens date from before the LGM, spanning major parts of MIS 3 and the earliest stages of MIS 2 (≈ 29-11 ka). This ~25 kyr time period was evidently favourable for the subsistence of mammoths, as implied by the recovery of mammoth remains up to 65°N latitude (Ukkonen et al., 1999; in prep.). The latest known occurrence of the mammoth before the LGM is recorded in Denmark to ~24 ka (Paper IV) – only a few thousand years prior to the maximum ice extent in the region (Houmark-Nielsen, 2004). Contrary to the previously widely accepted view of glacial history in Scandinavia, numerous dated ice-free deposits from Scandinavia (Arnold et al., 2002; Ukkonen et al., 2007; Helmens et al., 2007; Salonen et al., 2008) and ice sheet simulations (Arnold et al., 2002) indicate that the circum-Baltic mammoths with ages ca. 30 ka and older most likely lived during a time of a very limited ice sheet extent. The time period, corresponding to MIS 3, was marked by a highly unstable climate, evidenced as a series of rapid oscillations between cold stadial and warmer interstadial conditions called Dansgaard-Oeschger events (D/O) in ice core (Johnsen et al., 1992; Grootes et al., 1993), marine (e.g. Voelker et al., 1998) and terrestrial records (e.g. Allen et al., 1999; Genty et al., 2003).

Five mammoth specimens – four from the Baltic countries and one from Poland – date to the post-LGM period and the termination of the Weichselian ice age. The period is characterised by abrupt climatic transitions from the Oldest Dryas cold stage to the Bølling/Allerød interstadial at 14.7 ka, from the Allerød to the Younger Dryas cold spell at 12.9 ka, and from the Younger Dryas to the Holocene at 11.7 ka (Björck et al., 1998; von Grafenstein et al., 1999; Steffensen et al., 2008).

3.3.1 The $\delta^{18}O$ record – local variability and geographical patterns

The enamel-derived $\delta^{18}O_w$ values display significant intra-regional variation, with the higher end usually ~3‰ above the lowest regional value (Table 1; Paper IV). Interestingly, enamel samples from the Niederweningen mammoth accumulation in Switzerland (Tütken et al., 2007), tentatively correlated to the prominent and lengthy D/O event 12 (Furrer et al., 2007), also display a $\delta^{18}O_w$ variation of 3‰. This magnitude of variation can be induced by 'normal' year-to-year $\delta^{18}O_w$ variation in a steady state climate (Hoppe, 1999). However, the similarity of the regional $\delta^{18}O_w$ range to the amplitude of the stadial-interstadial oscillations in ice core records and terrestrial archives (Johnsen et al., 1992; von Grafenstein et al., 1999; Spötl and Mangini, 2002; Spötl et al., 2006) also allows an interpretation related to the D/O fluctuations (Paper IV). In this case, the mammoth data would provide valuable insights into the magnitude of the D/O events on the European continent. Although D/O oscillations have been recognised from diverse European terrestrial records of MIS 3 (Allen et al., 1999; Bar-Matthews et al., 2000; Spötl and Mangini, 2002; Genty et al., 2003; Moine et al., 2008), measurements of their precise magnitude in terms of $\delta^{18}O_{ppt}$ variations have been complicated by, e.g., the numerous different parameters influencing calcite $\delta^{18}O$ values in cave deposits (e.g. Spötl and Mangini, 2002; Genty et al., 2003).

3.3.1.1 Pre-LGM period

Long-term mean $\delta^{18}O_w$ values for each region, calculated using the pre-LGM specimens with finite dates suggest that glacial meteoric waters in northern Europe had $\delta^{18}O_{ppt}$ values ranging from -9.2±1.5‰ in western Denmark to -15.3‰ in northwestern Russia (Table 1). When the pre-LGM long-term mean $\delta^{18}O_w$ values are compared to the present-day $\delta^{18}O_{ppt}$ values (from Burgman et al., 1987;

Table 1. Mammoth enamel –derived $\delta^{18}O_w$ values and reconstructed mean annual palaeotemperatures.

		$\delta^{18}O_w$ (‰)		**palaeo-T (°C)**	**reference**
	min	**max**	**pre-LGM mean**	**pre-LGM mean**	
southern Finland			-14.2 (n=1)	-2 to -1	Paper I
eastern Finland			-14.6 (n=1)	-3 to -2	Paper I
northwestern Russia			-15.3 (n=1)	0	Paper I
central Sweden	-15.7	-12.6	-13.7±1.2 (n=3)	-1	Paper II
southern Sweden	-15.7	-12.8	-13.8±1.6 (n=3)	0 to -1	Paper II
western Denmark	-10.7	-7.7	-9.2±1.5 (n=2)	+3	Paper IV
eastern Denmark	-12.2	-11.7	-11.9±0.3 (n=3)	+3	Paper IV
Estonia	-15.4	-12.3	-13.9±0.6) (n=3)	-3 to -2	Paper IV
Latvia	-14.6	-11.7	-12.8±1.3 (n=4)	-2 to 0	Paper IV
Lithuania	-14.7	-11.7	-13.2±1.6 (n=4)	0 to +1	Paper IV
southern Poland	-12.7	-10.1	-11.9±0.5 (n=5)	+4	Paper IV
Data from prior mammoth enamel studies:					
southwestern Russia	-12.9	-11.5	-12.0±0.5 (n=7)	+1 to +2	Genoni et al., 1998
Switzerland	-13.8	-10.7	-12.3±0.9 (n=10)	+4	Tütken et al., 2007
western Germany	-9.8	-8.4	-9.1±0.7 (n=3)	+4 to +5	Tütken et al., 2008
North Sea	-9.2	-9.0	-9.1±0.1 (n=2)		Tütken et al., 2008
southern Britain	-9.0	-8.6	-8.8±0.2 (n=2)	+3	Ayliffe et al., 1992

Minima and maxima include all analysed specimens, the pre-LGM mean includes only those with finite dates 52-24 ka.The sample-specific $\delta^{18}O_w$ values and the regional δ/T slopes used to reconstruct the palaeotemperatures are given in Paper IV.

Punning et al., 1987; d'Obyrn et al., 1997; Kortelainen and Karhu, 2004; Kurita et al., 2004; IAEA/ WMO 2006; Zuzevičius et al., 2007), significant geographical differences in the magnitude of the glacial-to-modern change are displayed (Table 1 in Paper IV).

Prior $\delta^{18}O$ studies of European woolly mammoth tooth enamel dated to the late and middle Weichselian, compiled in Paper IV (data for Britain from Ayliffe et al., 1992; southwestern Russia from Genoni et al., 1998; Switzerland from Tütken et al., 2007; western Germany and the North Sea from Tütken et al., 2008), indicate that the $\delta^{18}O_{ppt}$ shift from glacial conditions to the present-day was 1-2‰ in southern Britain, the southern North Sea area, northern Switzerland and western Germany, and 3‰ in southwestern Russia (Fig. 4). Further information on the glacial-to-modern $\delta^{18}O$ change in Europe is available from oxygen isotope studies of palaeogroundwaters (Appendix in Paper IV; Rozanski, 1985; Stute and Deák, 1989; Bertleff et al., 1993; Le Gal La Salle et al., 1996; Darling et al., 1997: Beyerle et al., 1998; Dray et al., 1998; Poole, 1998; Hinsby et al., 2001; Huneau et al., 2002; Zuber et al., 2004), which in several locations indicate excellent comparability with local enamel-derived $\delta^{18}O_w$ estimates (Paper IV). Taken together, the mammoth enamel and the palaeogroundwater records suggest, that the $\delta^{18}O$ values of glacial waters in western and central Europe are 1-2 ‰ more depleted in ^{18}O relative to the oxygen isotope composition of present-day precipitation and groundwater recharge in the respective regions (Fig. 4). The larger shifts took place generally inland towards the east, and the <1.5‰ changes in the west.

Glacial-interglacial $\delta^{18}O$ shifts similar to those in central and western Europe are suggested by the new north European mammoth enamel data for Denmark, Poland, northwestern Russia and

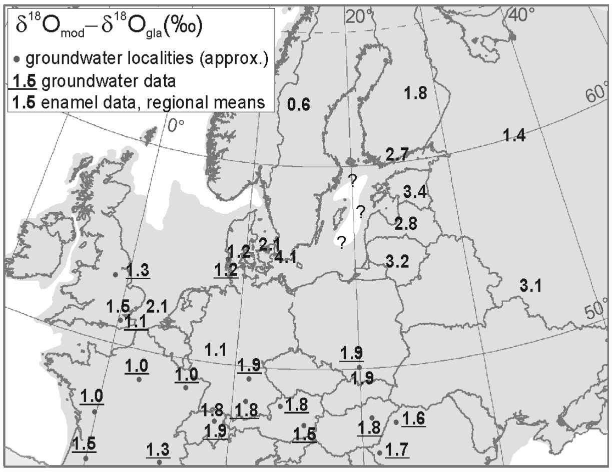

Figure 4. The difference (in ‰) between present-day $\delta^{18}O$ values of precipitation/groundwater and glacial (52-24 ka) $\delta^{18}O$ levels. The glacial values are based on regional means calculated from the mammoth enamel data and palaeogroundwater $\delta^{18}O$ values. The light grey coastline is -80 m below present sea level (Lambeck et al., 2002). The extent of waters in the Baltic basin is unknown.

eastern Finland (Fig. 4). In contrast, larger glacial-interglacial $\delta^{18}O$ differences of 3-4‰ are shown for regions near the present-day Baltic Sea coast and southwestern Russia close to the Ukrainian border (Genoni et al., 1998). In northern Europe around the Baltic Sea coast, the prominent ^{18}O depletion of glacial precipitation most likely reflects the significantly increased distance to marine moisture, brought about by the glacial lowstand of the global sea level (-80 m during MIS 3; Lambeck et al., 2002). During the middle Weichselian, the present-day low-gradient North Sea area between Britain and Denmark was drained and the coastline receded several hundred kilometres to the northwest, enhancing the isotopic distillation of westerly atmospheric moisture arriving in southern Fennoscandia and the Baltic countries. Further, it can be assumed that changes in the Baltic Sea status, supposedly a much smaller extent and a freshwater state, also affected the isotopic and moisture budget of the area. In southwesternδpasses.

Together with the compiled $\delta^{18}O_w$ values from previous investigations of mammoth enamel phosphate and the $\delta^{18}O$ values of late Pleistocene palaeogroundwaters (Appendix in Paper IV), the northern European enamel-derived $\delta^{18}O_w$ values facilitate a reconstruction of the geographic patterns of $\delta^{18}O_{ppt}$ values over much of Europe at 52-24 ka (Fig. 3 in Paper IV). However, the mammoth bioapatite $\delta^{18}O$ values produced in different laboratories employing various analytical techniques may not be fully comparable to each other (e.g. O'Neil et al., 1994; Vennemann et al., 2002; Lécuyer, 2004). As the use of different standard materials in the respective laboratories prevents the calibration of the dataset to a common standard, some isotopic offsets may occur. The matter is discussed in Paper IV. In regions where the number and/or temporal coverage of enamel samples is limited, e.g. Finland, there is an increased possibility of bias in the $\delta^{18}O_w$ taken to represent the long-term mean $\delta^{18}O_{ppt}$ value (see Clementz and Koch, 2001; Hoppe et al., 2005).

The overall spatial pattern resembles the present-day pattern of oxygen isotope ratios in precipitation: the highest $\delta^{18}O_{ppt}$ values occur in the southwest, and there is a progressive depletion towards the northeast (Fig. 2 and 3b in Paper IV). The glacial $\delta^{18}O_{ppt}$ values display a total range of -7 – -9‰ in coastal France and Britain to -14 – -16‰ in the Baltic countries, Sweden, Finland and northwestern Russia (Paper IV). A comparison of the modern and glacial regional oxygen isotope values shows a steepening in the north-south $\delta^{18}O$ gradient for the pre-LGM period below 60°N and east of ca. 10°E. This supports the view that a stronger latitudinal temperature gradient, perhaps linked to a southward shift of the polar front and jet stream, could be the reason for discrepancies between simulated vegetation and the proxy records of palaeovegetation (Alfano et al., 2003; Huntley et al., 2003). An intensified north-south gradient was also observed in marine surface temperatures derived from planktonic foraminiferal assemblages in the mid-latitude (40-50°N) North Atlantic at 40-20 ka (Chapman and Maslin, 1999). Additionally, the mammoth enamel data imply stronger west-east gradients relative to the present situation. In the latitude of the southern Scandinavian and

Lithuanian/Latvian mammoth localities, the longitudinal gradient in $\delta^{18}O_{ppt}$ values shows an almost twofold steepening from 2 to 3.8‰. On a west-east axis from Britain through the central European localities to southwestern Russia, the total change in $\delta^{18}O_{ppt}$ values amounts to ca. 3.2‰, which is double compared to the present-day variation of 1.6‰. The change occurs mostly between 0° and ~10°E, while the continental interior shows very little variation in the mean $\delta^{18}O_{ppt}$ values. Thus, it seems plausible that the southern seas supplied additional moisture to eastern Europe also during the glacial period, as determined for the present-day winter moisture budget in the area (Rozanski et al., 1993).

A palaeo- $\delta^{18}O_{ppt}$ contour map (Fig. 5b), drawn on the basis of the long-term enamel-derived and palaeogroundwater $\delta^{18}O$ data, shows a general pattern of the glacial $\delta^{18}O_{ppt}$ values over western and central Europe closely resembling the present-day pattern (Fig. 5a), but shifted to lower values by 2‰. To the northeast of the Alps, the geographic pattern of $\delta^{18}O_{ppt}$ is poorly defined. Data from the northern parts of Germany and Poland, the Czech Republic, Slovakia and Ukraine are needed to resolve the glacial $\delta^{18}O_{ppt}$ pattern in eastern Europe. Differences between the present-day and glacial patterns become apparent in northern Europe. Perhaps the most notable dissimilarity appears over Sweden. In contrast to the present-day situation, the glacial $\delta^{18}O_{ppt}$ pattern over the region virtually lacks north-south variation, as already discussed above.

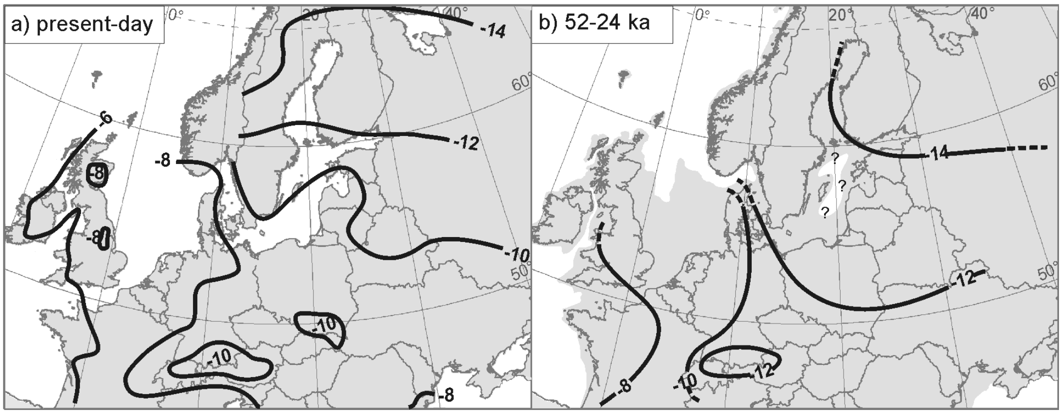

Figure 5. The spatial pattern of $\delta^{18}O$ in precipitation. **a)** Present-day situation, drawn based on Burgman et al. (1987), Darling et al. (2003), IAEA (2006) and Kortelainen (2007). **b)** Glacial pattern based on mammoth enamel regional mean values and palaeogroundwater oxygen isotope values. Palaeocoastline and Baltic Sea as in Fig. 4. Figure modified from Paper IV.

The large-scale glacial geographical $\delta^{18}O_{ppt}$ pattern reflects the progressive isotopic depletion of air masses moving northeast. Further, the circulation pattern appears to have remained essentially unaffected by the presence of an inland ice mass in the Scandinavian mountains. These observations agree with model simulations indicating a dominant strong westerly flow over the region during MIS 3, and that the SIS, within the size range plausible for the time period, had little impact on the climate of Europe during MIS 3 (Barron and Pollard, 2002; Pollard and Barron, 2003; van Meerbeeck et al., 2009). Isotopic evidence from glacial groundwaters first presented by Rozanski (1985) and expanded on by Darling (2004), showed that the atmospheric circulation pattern has remained essentially unchanged for the last 35 kyr over central Europe. The north European mammoth data now extend this argument both temporally, back to at least ca. 45 ka, and geographically to northern Europe ~64°N. While the compiled isotopic data set leaves room for improvement in both temporal and spatial coverage, the reconstructed palaeo-map of $\delta^{18}O_{ppt}$ is valuable for validation of atmospheric circulation models incorporating isotope tracers.

3.3.1.2 Post-LGM period

The mammoth enamel samples post-dating the LGM display $\delta^{18}O_w$ values (Table 2) in agreement with the major climatic fluctuations of the lateglacial period – the Younger Dryas stadial, the Bølling-Allerød interstadial and the Oldest Dryas stadial period.

The $\delta^{18}O_w$ values derived for the Oldest Dryas stadial period from the samples from Latvia and Lithuania, as well as the ~1000 years older enamel samples from Eliscevichi in southwestern Russia (Genoni et al., 1998) are 3-5‰ more depleted in ^{18}O relative to the present-day precipitation in these regions, consistent with cold stadial climatic conditions.

The calculated $\delta^{18}O_w$ value for the Oldest Dryas-Bølling transition and the beginning of the Bølling interstadial at 15.3-14.5 ka from Poland is 2‰ more positive than the regional long-term mean $\delta^{18}O_w$ value for the pre-LGM time period and is near the present-day regional $\delta^{18}O_{ppt}$ values.

The youngest specimens, the Puurmani molars from Estonia represent the Younger Dryas cold stage at 12.5-11.0 ka. They give a mean $\delta^{18}O_w$ value 5‰ below modern $\delta^{18}O_{ppt}$ compositions for the region. The low $\delta^{18}O_w$ value reflects cold climatic conditions, consistent with limnic and vegetational responses reported from adjacent western Russia, recording the Holocene warming only after 11.5 ka (Wohlfarth et al., 2007).

Table 2. Enamel-derived $\delta^{18}O_w$ values, mean annual palaeotemperature estimates, and the difference between estimated palaeotemperature and present-day mean annual surface temperature (ΔT) for the post-LGM period.

	age (ka)	**$\delta^{18}O_w$**	**ΔT (°C)**	**palaeo-T (°C)**	**reference**
southwestern Russia	18.0-16.5	-12.0	6-7	0-1	Genoni et al., 1998
Lithuania	17.1-16.9	-13.2	6-8	-1 to 0	Paper IV
Latvia	15.6-15.3	-14.6	10-12	-6 to -4	Paper IV
Poland	15.3-14.8	-10.1	2	6	Paper IV
Estonia	12.5-11	-15.3	9-10	-5 to -4	Paper IV

3.3.2 Palaeotemperature estimates from $\delta^{18}O$

Glacial palaeotemperatures over Europe were estimated based on the enamel $\delta^{18}O_w$ values from the circum-Baltic region (Papers I, II, IV), supplemented by data from previously published European mammoth enamel studies (Ayliffe et al., 1992; Genoni et al., 1998; Tütken et al., 2007; 2008).

Numerous studies indicate that long-term temperature trends have a dominating role in determining the oxygen isotope content of precipitation during past climates on a global scale (e.g. Rozanski et al., 1992; Cuffey et al., 1995; Jouzel et al., 1997; Fricke and O'Neil, 1999; Jouzel et al., 2000). Nevertheless, significant changes in the source conditions, vapour transport pathways, airmass boundary positions, recycling of moisture and the seasonality of precipitation may render the $\delta^{18}O$–temperature correlation determined for the present-day conditions inapplicable to reconstruct past climates (e.g. Fricke and O'Neil, 1999; Alley and Cuffey, 2001). Indeed, ice core measurements in Greenland have revealed significantly lower temporal gradients in $\delta^{18}O_{ppt}$ vs. temperature with respect to the present-day spatial relation (Cuffey et al., 1995; Johnsen et al., 1995). Yet, model simulations of LGM climate (Jouzel et al., 2000) indicate no robust tendency for lower temporal slopes globally, and glacial-interglacial temporal slopes close to present-day spatial gradients have been reported from North-America and Europe (e.g. Rozanski et al., 1992; Remenda et al., 1994; Edwards et al., 1996; Beyerle et al., 1998; Hammarlund, 1999; Zuber et al., 2004).

The atmospheric circulation pattern and rainout process, as well as the $\Delta^{18}O/\Delta T$ associated with the transition from glacial to interglacial climate (=temporal δ/T slope) has been relatively well studied in western and central Europe using the stable isotope ratios and the noble gas contents in late Pleistocene groundwaters (e.g. Rozanski, 1985; Darling et al., 1997; Huneau et al., 2002; Darling, 2004). These investigations have shown that vapour transport and rainout have remained virtually unchanged from the glacial period to the present interglacial. Further, the studies indicate that there is considerable geographical variation in the Pleistocene-to-Holocene temporal δ/T-gradients. Temporal δ/T-slopes are here defined to include the difference between the mean glacial and the modern recharge $\delta^{18}O$ values, taking into account the ^{18}O enrichment in the glacial oceans. In coastal and western Europe the δ/T-slopes are ca. 0.3-0.4‰/°C (Darling et al., 1997; Dray et al., 1998; Hinsby et al., 2001; Huneau et al., 2002), while central Europeans localities, especially in higher altitudes, typically display higher temporal gradients (Rozanski et al., 1992; Loosli et al., 2001) with slopes of ~0.5-0.7 (Andrews et al.,1985; Stute and Déak, 1989; Bertleff et al., 1993; Beyerle et al., 1998; Zuber et al., 2004). The latter gradients are similar to the relation for the decadal-scale changes in T and $\delta^{18}O_{ppt}$ (0.63‰/°C), as well as the average present-day spatial slopes (0.59‰/°C) in continental Europe (Rozanski et al., 1992) and in high-latitude coastal areas (0.69‰/°C; Dansgaard, 1964). To interpret temperature shifts associated with the mammoth $\delta^{18}O_w$ data, geographically varied regional estimates for temporal δ/T slopes ranging from 0.3 in western Europe to 0.7 in the east (Paper IV) were used. However, the exact calibration of the δ/T relationship for glacial times is not empirically known in all regions, and thus, the calculated temperature shifts and palaeotemperatures should be viewed with caution.

3.3.2.1 Intra-regional temperature variability

If attributable solely to temperature changes, the 3‰ intra-regional variability in enamel-derived $\delta^{18}O_w$ values implies 5-7°C regional temperature differences between the cold and warm climate states. For comparison, ice core data imply D/O-associated temperature fluctuations from 7°C (Johnsen et al., 1992) up to 12-15°C (Johnsen et al., 2001) for Greenland. The smaller temperature changes suggested by the mammoth data are logical considering observations of a stronger temperature shift in Greenland compared to mid-Europe (von Grafenstein et al., 1999). In contrast, the latest MIS 3 –focussed modelling efforts (van Meerbeeck et al., 2009) indicate less than 1°C difference for the simulated stadial and interstadial climates. The coldest single episodes represented by the mammoth enamel data, recorded in Sweden and Latvia, indicate temperatures 10-13°C below the regional present-day values. For some of the warmer periods, the enamel data imply temperatures from 0°C (central Sweden) to 2°C (Denmark, Switzerland, Germany) below the modern levels.

3.3.2.2 Pre-LGM thermal climate

The enamel-derived $\Delta^{18}O$ shifts (including the glacial ocean effect) indicate geographically variable differences in the mean annual temperatures (ΔT) between the long-term glacial and the present-day conditions. The inferred temperature differences vary from 2 to 9°C, both ends of the spectrum describing the glacial-interglacial change in the thermal climate in Sweden. The inferred ΔT ranges translate to pre-LGM long-term mean annual temperatures between -3°C and 5°C. The spatial distribution of the inferred pre-LGM palaeotemperatures, along with glacial recharge temperatures derived from noble gas contents of Late Pleistocene groundwaters, is shown in Figure 6. With implied mean annual temperatures below 0°C for Sweden, Finland, the Baltic countries and northwestern Russia, and 1-5°C for southwestern Russia, Denmark, southern Britain, Switzerland and southern Poland, the data imply a position for the 0°C isotherm from southern Sweden across the Baltic basin towards Lithuania and northwestern Russia (Fig. 6).

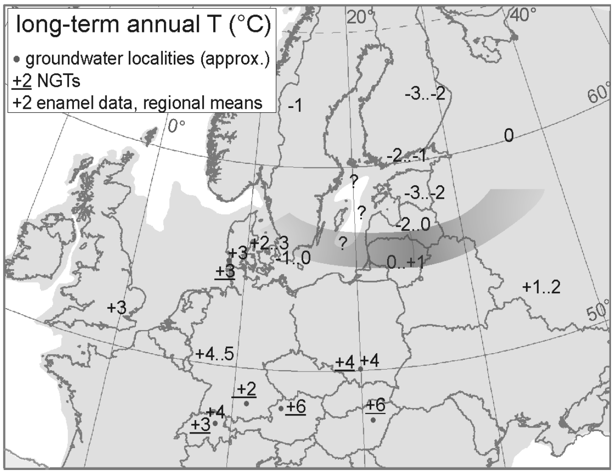

Figure 6. Long-term palaeotemperatures for the glacial period 52-24 ka. The values reconstructed from the regional mammoth enamel $\delta^{18}O_w$ values are long-term average values of mean annual temperatures; the palaeogroundwater data are noble gas recharge temperatures (NGTs). Shaded grey sector represents the approximate location of the 0°C isotherm. Palaeocoastline as in Fig. 4.

The validation of the enamel-derived temperature estimates is made difficult by the limited amount of palaeotemperature data existing for the pre-LGM period in Europe. However, they agree reasonably well with those calculated from noble gas concentrations in palaeogroundwaters from regions not used in the estimation of the temporal δ/T-slopes (e.g. Rozanski, 1985; Dray et al., 1998) and those inferred from model simulations (van Huissteden et al., 2003). The palaeotemperature estimate of ~ -1°C for central Sweden, close to the modern mean annual surface temperatures in the region, is supported by MIS 3 coleopteran assemblages from the Pilgrimstad interstadial deposit in the same area (Robertsson, 1988; Johnsen et al., 2008). They indicate annual mean maximum and minimum temperatures (T_{max}=10°C, T_{min}= -10°C; Moseley, 1982, cited by Ambrosiani and Robertsson, 1992) very similar to modern January and July temperatures in the region (1961-1990 mean T_{max}=11-14°C, T_{min}=-7 to -11°C; Vedin, 2007). Taken together with the palaeobotanical and –zoological evidence of near present-day temperatures during the early MIS 3 in Sokli, northern Finland (Helmens et al., 2007; Engels et al., 2008; Bos et al., 2009), the $\delta^{18}O_w$ data for the Swedish uplands suggests that the general cooling associated with MIS 3 might have been relatively minor in the higher latitudes of western Europe.

In contrast, fossil beetle faunas and widespread periglacial features in northwestern Europe (e.g. Huijzer and Vandenberghe, 1998; Kasse et al., 1998; Coope, 2002; van Huissteden et al., 2003) bear evidence of severe cold spells, during which temperatures could reach near-LGM levels (van Andel, 2002). The periglacial features require very low mean annual temperatures to form, estimates ranging from -8 to -2°C (van Huissteden et al., 2003 and references therein). According to the mammoth data, long-term surface temperatures below -2°C are reached only in eastern Finland and Estonia. If individual data points are considered instead of regional averages, the coldest inferred temperatures during the pre-LGM period, from -4 to -3°C, are recorded in Sweden, Latvia and Estonia. In central and western Europe the pre-LGM mammoth record lacks traces of such cold climatic extremes, and they are not reproduced by regional MIS 3 climate simulations for Europe (Barron and Pollard, 2002; van Huissteden, 2003; Pollard and Barron, 2003) or by the most recent global MIS 3 climate modelling study (van Meerbeeck et al., 2009). Evidently, the severe cold spells were of short duration, in the order of one to a few decades, and thus do not represent average MIS 3 conditions (van Huissteden et al., 2003).

3.3.2.3 Post-LGM thermal climate

The few mammoth specimes post-dating the LGM give approximations of the palaeotemperatures during the lateglacial climatic phases (Table 2). The post-LGM phase includes the lowest recorded mean annual temperatures, ~-6 – -4°C, obtained from Latvia and Estonia, representing the regional thermal climate of the Oldest Dryas and Younger Dryas cold spells.

Considering the uncertainties in the temporal $\delta^{18}O$-T gradients discussed earlier, the enamel-derived temperature estimates, listed in Table 2, are remarkably similar to the palaeotemperatures derived by Renssen and Isarin (2001) from modelling and compiled proxy data for the respective areas of the mammoth find localities. The 9-10°C lower mean annual temperature inferred for the Younger Dryas cold stage in Estonia also agrees with Birks and Ammann (2000), reporting 8-10°C and 12-13°C lower summer temperatures for Switzerland and Norway, respectively. Furthermore, considering the observations of 1.5-fold temperature changes in Greenland relative to Europe (von Grafenstein et al., 1999), the Younger Dryas –associated temperature change in Estonia is in line with the 15°C lower surface temperatures inferred for the Greenland summit at the time (Severinghaus et al., 1998; Alley, 2000). On the other hand, the dramatic temperature shifts recorded in western Europe and Greenland are in contrast with that inferred for the northern Urals, where summer temperatures were only ~1°C below the present-day levels during the Younger Dryas (Väliranta et al., 2006). The more prominent manifestation of the Younger Dryas in northwestern Europe evidently reflects the strength of the influence of the North Atlantic Ocean, the key area for shifting climate regimes in Greenland and Europe (e.g. von Grafenstein et al., 1999; Alley, 2000; Steffensen et al., 2008).

3.3.3 The $\delta^{13}C$ record

This chapter includes previously unpublished results from mammoth enamel $\delta^{13}C$ analyses on specimens from Latvia, Estonia, Lithuania, Poland and Denmark, performed on the same samples as the $\delta^{18}O$ analyses reported in Paper IV. The new data show $\delta^{13}C$ values from -12.7‰ to -10.7‰ (Table 3), in good agreement with the mammoth enamel $\delta^{13}C$ values from Finland and adjacent northwestern Russia (Paper I), Sweden (Paper II) and Switzerland (Tütken et al., 2007). The discussion is based on a combined data set of the European mammoth enamel $\delta^{13}C$ values from these regions. Specimens with infinite ^{14}C dates are excluded.

In contrast to the $\delta^{18}O$ values, the $\delta^{13}C$ data indicate relatively small within-region variation, ranging from 0.6 to 1.2‰. Samples from Latvia have the lowest mean value of -12.4±0.3‰ and those from Denmark the highest mean value of -11.2± 0.5‰. The two specimens from Finland show low $\delta^{13}C$ values below -12‰, and the single sample from Kirillov, northwestern Russia, has a $\delta^{13}C$ value of -11.2‰. The Polish, Swedish, Lithuanian and Estonian specimens give intermediate regional mean values at -11.3±0.4‰, -11.4±0.4‰, -11.5±0.3‰ and -11.6±0.4, respectively. The mean $\delta^{13}C$ value of the mammoth enamels from northern Switzerland at -11.5±0.3‰ (n=10) (Tütken et al., 2007) is similar to these.

The European mammoth enamel $\delta^{13}C$ values are typical of herbivores in pure C3 ecosystems. According to the apatite-diet offsets at ~14‰ displayed by modern ungulates (Cerling and Harris, 1999; Cerling et al., 1999), the vegetation preferred by the European mammoths had $\delta^{13}C$ values from -24.6 to -27.2‰. Factoring in the ~0.5-1‰ higher $\delta^{13}C$ values of glacial atmospheric CO_2 (section 1.2.3; Marino et al., 1992), these values are fully comparable to modern plants using the C3 photosynthetic pathway.

The geographic distribution of the enamel $\delta^{13}C$ values is shown in Figure 7. A faint geographic trend is discernible, with lower values more frequent in the northeast. The $\delta^{13}C$ values have a weak but significant negative correlation with longitude ($r= -0.32$, $n=47$, $p<0.05$), which improves ($r= -0.40$, $n=46$, $p<0.01$) if the only available value from the easternmost location (Kirillov, Russia; 38°E) is removed. The strength of the negative correlation with latitude is similarly weak, but significant. The coefficient of determination does not improve if both longitude and latitude are used as independent variables. Adopting a correction of -0.5‰ to scale down the $\delta^{13}C$ values of the lateglacial samples to the level of atmospheric CO_2 $\delta^{13}C$ values of the full glacial samples (e.g., Koch et al. 1998), the correlations remain essentially the same.

Table 3. Carbon isotope composition (δ^{13}C) of the mammoth enamels from Denmark, the Baltic countries and Poland.

Locality	^{14}C lab no. [a]	^{14}C yr BP	Calendar age [b] 95% range	δ^{13}C (‰)
Denmark				
Hornbæk	LuS 7414	22900 ± 150	28.5-27	-10.6[f]
Højballegård, Hansted	LuS 7415	19940 ± 120	24-23.5	-11.7
Nymølle, Sjælland	K-6000[c]	34640 ± 1830	43-34.5	-11.5[f]
Høgebjerg	LuS 7416	26400 ± 200	32-30.5	-10.8
Nymølle, Sjælland	K-5999[c]	26060 ± 1070	32.5-29	-11.3[f]
Estonia				
Puurmani-Laeva	Hela-423[d]	10100 ± 200	12.5-11.0	-11.9[f]
Valga	OxA-11607[e]	28780 ± 160	34-32.5	-11.1
Kallaste, Saru	Hela-421[d]	>38000	>41.5	-11.3[f]
Mooste, Kaaru	Hela-418[d]	30640 ± 830	36-33.5	-11.8
Puurmani, Saare-Utsali	Hela-425[d]	10200 ± 100	12.3-11.4	-12.1
Ihasalu	Hela-426[d]	>41000	>42.5	-11.8[f]
Koosa	OxA-12058[e]	40900 ± 600	45.5-43	-11.3
Latvia				
Ikšķile, Ogre district	LuS 7535	40850 ± 750	46-42.5	-12.4
Pļaviņas, Aizkraukle district	LuS 7536	27850 ± 200	33-32	-12.1
Jaunpils, Tukums district	LuS 7537	40700 ± 800	45.5-42.5	-12.5
Rucava, Liepāja district	LuS 7538	12875 ± 70	15.6-15.3	-12.1[f]
Veselava, Cēsis district	LuS 7539	25800 ± 170	31.5-30	-12.7[f]
Lithuania				
Jonava region, Turžėnų	LuS 7528	21400 ± 120	26-25	-11.2
Kaunas region, river Jiesia	LuS 7529	13800 ± 80	17.1-16.9	-11.6[f]
Skermentiškių	LuS 7530	no collagen		-11.8
Kaunas region, river Jiesia	LuS 7531	42300 ± 1000	47.5-43.5	-11.3[f]
Kaunas region, river Jiesia	LuS 7532	41350 ± 800	46.5-43	-11.7
Telšiai region, Pilsūdai	LuS 7533	33650 ± 300	42-35.5	-11.1[f]
Poland				
Kraków Spadzista Street B	LuS 7417	23750 ± 150	29-28	-11.5[f]
Kraków Spadzista Street C2	LuS 7418	23750 ± 150	29-28	-10.9[f]
Kraków Spadzista Street E	LuS 7419	24700 ± 180	30-29.5	-10.7
Kraków Spadzista Street F	LuS 7420	24625 ± 180	30-29	-11.3
Kraków Zwierzyniec		no date		-11.6[f]
Kraków Zwierzyniec	LuS 7421	22800 ± 150	28-27	-11.1
Dzierżysław	LuS 7422	10510 ± 70[g]	12.8-12.1[g]	-11.9
Dzierżysław	LuS 7739	12585 ± 70	15.3-14.8	

[a] Samples with prefix LuS: Paper IV. [c] Aaris-Sørensen, 2006; [d] Lõugas et al., 2001; [e] Lister and Stuart, unpublished (funded by the Natural Environment Research Council, UK, performed at the Oxford Radiocarbon Accelerator Unit through Dr. Tom Higham)

[b] Calibration after Weninger and Jöris (2008)

[f] Mean of two analyses

[g] Low carbon content in collagen, age may appear too young.

In a strictly C3-based environment such as glacial Europe, the observed geographic trend in the enamel $\delta^{13}C$ values probably reflects $\delta^{13}C$ variations in the consumed plants caused by environmental parameters (e.g. Heaton, 1999) in a similar manner as that reported for the Holocene by van Klinken et al. (1994). The $\delta^{13}C$ values of Holocene bone collagen and plant material in Europe show a distinct climate-induced geographic pattern, with strong and very highly significant correlations to air temperature and humidity (van Klinken et al., 1994; 2000).

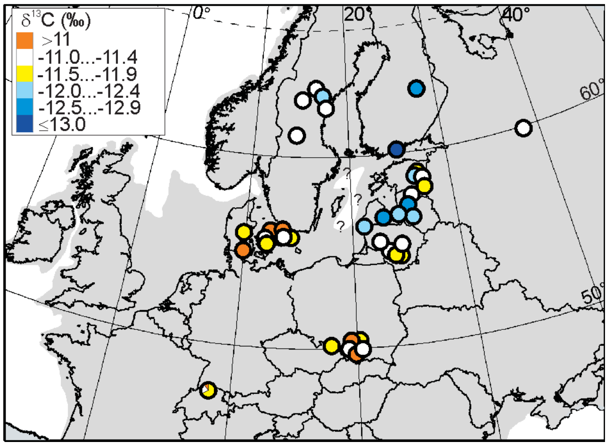

Figure 7. Geographic distribution of $\delta^{13}C$ values in mammoth enamel 52-11 ka, with no correction for the changes in $\delta^{13}C$ values of atmospheric CO_2. Palaeocoastline as in Fig. 4.

A variety of environmental factors, inducing changes in plant stomatal conductance and carboxylation rate, affect the $\delta^{13}C$ values of C3 plants, and hence, herbivores. These factors are comprehensively reviewed by Heaton (1999). On a regional scale, the light intensity and temperature of the growth environment are positively correlated with the plant $\delta^{13}C$ values, whereas increases in humidity or water availability cause a decrease in the plant $\delta^{13}C$ values. Apart from being influenced by these environmental factors, geographical variations in C3 plant $\delta^{13}C$ levels are brought about by isotopic differences between plant species, forms and habitat types (Heaton, 1999). The effects of light and moisture availability combined with the recycling of isotopically light CO_2 from decomposing organic matter cause plants growing under dense forest canopies to have as much as 5‰ lower $\delta^{13}C$ values than those growing in open environments (e.g. van der Merwe and Medina, 1989; Heaton, 1999). This "canopy effect" is passed on to the herbivores resulting in lower $\delta^{13}C$ levels in animals feeding in more closed habitats (van der Merwe and Medina, 1991; Iacumin et al., 1997; Bocherens et al., 1999; Drucker et al., 2003; 2008).

The observed geographical distribution of the enamel $\delta^{13}C$ values could thus be interpreted to reflect higher water availability, lower humidity and temperatures, differences in consumed plant species/forms, or more closed habitats in the east compared to the more western regions. Whereas little information is available on the geographical variations in water availability or humidity during the glacial time period, the oxygen isotope data (Paper IV) from the same specimens provide information on temperature gradients in the area. The progressive lowering of oxygen isotope values toward the northeast (Fig. 2 in Paper IV) is consistent with lower temperatures in that direction (Fig. 6). Somewhat surprisingly, though, there is no significant correlation between the $\delta^{13}C$ and $\delta^{18}O_w$ values in each sample. The influence of surface temperature on the $\delta^{13}C$ values is reflected by a correlation ($r=0.61$, $p<0.05$, $n=10$) between the regional mean values of $\delta^{13}C$ and the palaeotemperatures reconstructed from the $\delta^{18}O_w$ values (Paper IV). The $\delta^{13}C$ values also correlate with the palaeotemperature values in each sample ($r=0.33$, $p=0.01$, $n=47$). Therefore, the glacial surface temperature gradient is probably one factor attributing to the observed geographical $\delta^{13}C$ pattern.

Additionally, support for an interpretation of differences in habitat openness is provided by palaeobotanical evidence, pointing toward more closed vegetation in the east. Pollen and macrofossil records from central Europe indicate predominantly treeless landscapes, with dwarf-shrub tundra, steppe tundra/warm steppe, or grassland as the main vegetation type north of the Alps during MIS 3 (e.g. Bos et al., 2001; Huntley et al., 2003). In northeastern Europe biomes during MIS 3 were characterised by low-arctic tundra in the north and boreal forests/taiga in the east (Gaigalas et al., 1992; Molodkov et al., 2007; Satkūnas et al., 2003; Bos et al., 2009; Davydova and Servent-Vildary, 1996; Huntley et al., 2003; Markova et al., 2003). The existence of more closed habitats towards the east could also potentially imply regional differences in the diet of the animals. Direct evidence of the mammoth diet in Siberia and North America, based on the composition of dung and the gastrointestinal contents of carcasses preserved in permafrost, indicates that it was largely based on grasses and sedges, and included variable amounts of mosses, herbs, and twigs of trees and shrubs (Vereschagin and Baryshnikov, 1982; Ukraintseva, 1986; Guthrie, 1990; Mead et al., 1986; van Geel, 2008). Assuming European mammoths had similar preferences, it could be hypothesised that the relative proportion of woody plant material in the mammoths' diet was smaller in the southwest compared to the northeast. However, observations of generally higher $\delta^{13}C$ values in arboreal vegetation compared to herbaceous plants (Heaton, 1999) argue against such a hypothesis. The $\delta^{13}C$ values of woody plants also display significant internal spatial variation with height from the ground, so that in the level most likely sampled by the mammoths, values are more negative than the mean values of the entire plant. In conclusion, the carbon isotope data alone cannot provide decisive answers to the hypotheses regarding regional differences in the composition of the diet.

A similar pattern of more negative $\delta^{13}C$ values in the northeast was also observed in the $\delta^{13}C$ values of mammoth collagen from the Russian plain and Siberia (Iacumin et al., 2000). A combined influence of differences in temperature, water stress and plant availability was found as the most likely reason accounting for the variation. Similarly, it is concluded that the pattern of European mammoth enamel $\delta^{13}C$ values most likely reflects a combination of the discussed environmental factors, and the geographic variation cannot be assigned to a single mechanism.

Apart from spatial variations, animal and plant $\delta^{13}C$ values have been shown to display a temporal trend characterised by declining isotope values towards the end of the Pleistocene epoch (Krishnamurthy and Epstein, 1990; Leavitt and Danzer, 1992; Hatté et al., 1999; Richards and Hedges, 2003; Hedges et al., 2004; Stevens and Hedges, 2004; Drucker et al., 2008), attributed to an increased canopy-effect caused by the expansion of forests at the Pleistocene-Holocene transition (Drucker et al., 2008), or to the rising atmospheric concentration of CO_2 (e.g. Hatté et al., 1999; Richards and Hedges, 2003; Hedges et al., 2004).

In order to study the potential long-term temporal trends in the European mammoth data, the effects of geographic, climate-related factors need to be eliminated. Stuiver and Braziunas (1987) reported a strong latitudinal dependency of 0.16 ‰ $°\text{latitude}^{-1}$ in wood cellulose $\delta^{13}C$ values in North America. The more negative isotope values with increasing latitude were related to variability of temperature and humidity, with very similar correlations to those observed between European bone and wood $\delta^{13}C$ values and climatic controls (van Klinken et al., 1994). The latitudinal correction can be applied to normalise samples to a common latitude to facilitate comparisons (e.g. Leavitt and Danzer, 1992).

When the mammoth enamel $\delta^{13}C$ data are normalised to an arbitrary latitude of 55°N using the coefficient suggested by Stuiver and Braziunas (1987), on average the lateglacial samples appear to display lower values than the pre-LGM samples (Fig. 8). However, the gradient is less obvious than the pattern seen in the $\delta^{13}C$ values of organic matter in the central European loess deposits (Hatté et al., 1999) or of mammal bones from northwestern Europe (Richards and Hedges, 2003) (Fig. 8), and the difference in the latitude-normalised mean values between the pre- and post-LGM mammoth samples is only significant at the 90% level (t-test: $0.05 < p < 0.1$). This might be expected as the European mammoth enamel $\delta^{13}C$ data has a rather poor coverage during the post-LGM period: Holocene samples are absent and the number of lateglacial specimens is small. Additionally, the mammoth samples originate from an extensive area with significant climatic variability, which the latitude-nomalisation procedure is evidently unable to entirely remove.

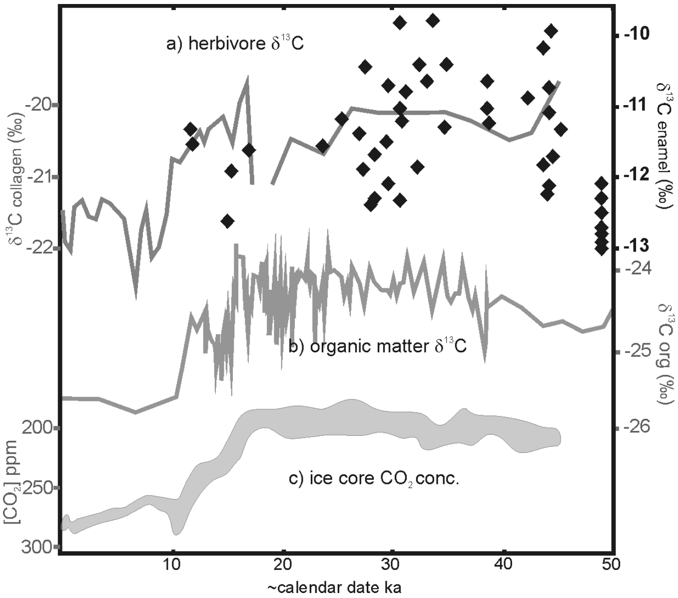

Figure 8. The temporal variation of a) $\delta^{13}C$ values of 'latitude corrected' mammoth enamel samples (black diamonds) and herbivore collagen from northwestern Europe (gray line and scale; Richards and Hedges, 2003), b) $\delta^{13}C$ values of organic matter from Nußloch, central Europe (Hatté et al., 1999), c) and concentration of CO_2 in Greenland and Antarctic ice cores (from Richards and Hedges, 2003; note the inverted scale).

In addition to the latitude-correction procedure, an approach based on the local July mean temperatures (van Klinken et al., 2000) was attempted, but it resulted in little change of the primary enamel $\delta^{13}C$ values and the relative position of the data points on a $\delta^{13}C$-calendar age diagram. The apparent insufficiency of the correction procedures (Stuiver and Braziunas, 1987; van Klinken et al., 2000) most likely arises from their calibration, which is based on modern climatic gradients. According to the oxygen isotope data, the glacial climate in Europe was characterised with steeper north-south and west-east climatic gradients in some parts, and a significant weakening of the present-day gradients in others. Further, the latitude-based procedure does not account for the climatic effects caused by altitude and the increasing continentality with longitude. These considerations suggest that the climate correction procedures do not necessarily produce meaningful 'corrected' $\delta^{13}C$ values for fossil specimens, especially if past climatic gradients significantly different from the modern ones can be expected.

3.4 Wrangel Island during MIS 3 to 1 – the lay of the land

The European palaeoenvironmental record in mammoth bioapatite ends at the final cold stage of the Weichselian ice age, the Younger Dryas at ca. 11 ka. The date also marks the extinction of the species in continental Eurasia (Stuart et al., 2002). On Wrangel Island, an isolated population of woolly mammoths survived until 4 ka (Vartanyan et al., 1993; 1995; Karhu et al., 1998) extending the palaeoenvironmental record late into the Holocene. The isotopic record in the skeletal remains of the woolly mammoths and other sympatric animals (bison, musk ox) holds evidence of two large-scale palaeoenvironmental changes: the transition from the ice age climate to the interstadial conditions, and the altered geography brought about by the eustatic rise of global sea level.

3.4.1 The $^{87}Sr/^{86}Sr$ record

During the late Pleistocene lowstand of the global sea level, the present-day Wrangel Island was an elevated region surrounded by the expansive shelf area now submerged in the Chukchi Sea. During the maximum Weichselian regression, the sea level fell 120-130 m below today's surface level (Fairbanks, 1989; Lambeck et al., 2002). As the melting of the ice sheets at the end of Pleistocene began to raise the global sea level, the connection to the mainland was gradually lost. Estimates of the island's separation range from ca. 14 ka (Vartanyan et al., 1993) to 10 ka (Saarnisto and Karhu, 2004). This process, affecting the ranging patterns of the local animals, is reflected in the $^{87}Sr/^{86}Sr$ ratios of skeletal remains discovered on the island.

The $^{87}Sr/^{86}Sr$ ratios of the bioapatite samples dated to the terminal Pleistocene have a significantly lower mean value (0.71218±0.00103, n=18) than that of the Holocene samples (0.71491±0.00138, n=27) or the recent samples (0.71431±0.00073, n=5), which are statistically indistinguishable from each other (Paper III). The samples of surface waters, expected to reflect the $^{87}Sr/^{86}Sr$ values of the bedrock units in the watershed (Graustein, 1989; Miller et al., 1993; Blum et al., 1993), show a range of environmental Sr isotope compositions comparable to those in recent reindeer and muskox bioapatite (Table DR1 and Fig. 2 in Paper III). Most of the Holocene mammoth bioapatite $^{87}Sr/^{86}Sr$ ratios also fall within the surface water range, but a few samples show even more radiogenic values. The direct implication of the observed differences in $^{87}Sr/^{86}Sr$ values is that the Pleistocene animals consumed plants growing on less radiogenic substrates than the Holocene mammals. Two possibilities arise: Either the Sr-isotope ratios of the plants on Wrangel Island changed, e.g., due to an increase in eolian dust flux during the Pleistocene cold phases, as documented in the polar ice sheets (e.g. Svensson et al., 2000). Or alternatively, the animals ranged in regions with different geological sources of $^{87}Sr/^{86}Sr$.

As the Sr isotopic composition of continental dust from East Asia, the dominant dust source at high northern latitudes during the late Pleistocene glaciations (Svensson et al., 2000; Yokoo et al., 2004; Sun, 2005; Tanaka and Chiba, 2006), is relatively high (0.714-0.718; Sun,2005; Tanaka and Chiba, 2006), its possible increased flux during the late Pleistocene would not have acted to produce lower $^{87}Sr/^{86}Sr$ values of the soil and plants on Wrangel Island. Thus, it is most likely, that the significant difference in the mean Sr isotope values of the terminal Pleistocene bioapatite relative to the Holocene and recent mammal remains indicates different feeding areas for the animals.

Whereas no direct measurements of the $^{87}Sr/^{86}Sr$ values in the geological formations on Wrangel Island or the now-inundated shelf areas are available, general conclusions can be drawn based on the type and age of the bedrock. On Wrangel Island, the oldest rocks are represented by the Neoproterozoic Wrangel Complex. The complex crops out in the central mountains, and could serve as a source of radiogenic ^{87}Sr . Geochemical analyses of leucogranites and acidic volcanites of the Wrangel Complex indicate that these rock types can contain 110-183 ppm Rb (Kos'ko et al., 1993), and can be expected to produce $^{87}Sr/^{86}Sr$ ratios as high as 0.776 (Paper III). The continental shelf surrounding Wrangel Island is composed of Lower Cretaceous to Tertiary sedimentary basins separated by positive features (Kos'ko et al., 1993). The Phanerozoic sedimentary terrains of the Chukchi shelf and Chukotka are assumed to have relatively low $^{87}Sr/^{86}Sr$ ratios due to the influence of marine limestones. Late Silurian– Late Permian limestones in the Palaeozoic sedimentary strata, which form much of the Chukchi shelf basement and are exposed on Wrangel Island and the Chukotkan coast (Huh et al., 1998; Viscosi-Shirley et al., 2003), are expected to reflect the $^{87}Sr/^{86}Sr$ ratios of contemporaneous seawater (~0.7070–0.7088; McArthur et al., 2001). Thus, in view of the general bedrock geology and the present-day reference Sr data available from Wrangel Island, it is plausible that the relatively low $^{87}Sr/^{86}Sr$ ratios of the terminal Pleistocene mammals are a reflection of feeding areas on the now inundated shelf area. Accordingly, the more radiogenic Sr isotope compositions of the mid-Holocene and recent remains reflect ingestion of Sr with higher $^{87}Sr/^{86}Sr$ ratios released by the Late Proterozoic Wrangel Complex rocks. This further implies that the terminal Pleistocene animals discovered from Wrangel Island were not local residents, but probably visited the area only occasionally. This is in agreement with conclusions of Vartanyan et al. (2008). Based on the frequency distribution of mammoth radiocarbon data, which they interpret to be primary (not an artifact of differential preservation) and directly proportionate to the concentration of resident animals, they suggest that the late Pleistocene mammals used the area of the present-day island for summer visits only.

The underlying reason for the change in the ranging behaviour of the animals was evidently a change in the palaeogeography of the area, induced by steadily rising sea levels at the end of the Pleistocene epoch. According to reconstructions based on sea floor topography and eustatic sea level curves, the connection to the mainland was flooded sometime between 14.7-13.9 ka (12-12.5 ^{14}C kyr BP; Vartanyan et al., 1993; Lozhkin et al., 2001) and 10-10.5 ka (Manley, 2002; Saarnisto and Karhu, 2004). Elias et al. (1996) argued that the sea level reached the -40 m isobath, equivalent to the critical depth of the connection between Wrangel Island and the mainland, at ca. 12.5 ka. The bioapatite Sr isotope data support shore line reconstructions placing the time of isolation to ~10–10.5 ka but can not conclusively rule out an earlier separation date of ~12.5 ka due to the lack of skeletal remains from that period. However, it seems unlikely that the -40 m depth would have been reached already at ~14-14.7 ka, as the bioapatite ^{87}Sr/^{86}Sr ratios of that time are indistinguishable from those of other terminal Pleistocene samples.

The ^{87}Sr/^{86}Sr record in the skeletal remains also allow for details of the isolation process to be detected. The mean Sr isotope ratios of samples dated to 8-6 ka and 6-4 ka are statistically alike, but the samples dated to 10-8 ka have a significantly lower mean ^{87}Sr/^{86}Sr ratio (t-test: $p < 0.05$) reflecting the situation soon after the separation, when the early Wrangel Island comprised extensive parts of the presently inundated shelf area. The timing of the gradual rise in the ^{87}Sr/^{86}Sr compositions of bioapatite is consistent with the Beringian bathymetric coast line reconstruction presented by Manley (2002), where

1) the connection to the mainland is lost between 11 and 10 ka; at 10 ka the sea level was at -36 m, and considerable areas of the shelf were part of the island (Fig. 3a-b in Paper III)
2) at 9–8 ka the sea level rose from -22 to -14 m, and the surface area of Wrangel Island was much reduced; at 8 ka the island's coastline was already very close to its present-day position (Fig. 3c-d in Paper III),
3) at 7 ka (-6 m) the island had assumed its present-day form.

The trend of mammoth bioapatite Sr ratios getting more radiogenic after 8 ka can be interpreted to reflect the rapid shrinking of the available range area at 10–8 ka, after which the animals had to inhabit less accessible, more mountainous regions of the island.

3.4.2 The δ^{18}O record

The oxygen isotope ratios of the mammoth bioapatite, reported by Karhu et al. (1998) and Saarnisto and Karhu (2004), track the climatic changes that happened concurrently with the regional palaeogeographical changes. The $\delta^{18}O_w$ values inferred from the Holocene samples are ca. 5‰ above those derived from the late Pleistocene samples, most of which date to MIS 2, i.e. the LGM sequence. The isotopic shift is of comparable magnitude to that of the Pleistocene-Holocene transition in the Greenland ice core δ^{18}O profiles (e.g. Johnsen et al., 2001), and in the central Arctic ice caps of the Severnaya Zemlya archipelago (Stiévenard et al., 1996). The large isotopic shift, 1-4‰ larger than the ones observed in Europe (Paper IV), reflects a significant change in the climate across the Pleistocene-Holocene transition. Using a δ^{18}O-T relationship of 0.69‰/°C (Dansgaard, 1964), Saarnisto and Karhu (2004) estimated a ~7°C increase in surface temperature on Wrangel Island across the Pleistocene-Holocene transition.

Along with changes in mean annual temperatures, the large isotope shift very likely also reflects the dramatic change in the lay of the land in a similar manner discussed, e.g., for southernmost

Sweden in Europe. At the time of the sea level's maximum regression the shoreline of the Arctic ocean was ca. 200 km to the north and northeast of the present-day Wrangel Island, and the Bering Sea in the southeast was drained. The extensive sea-ice cover would have further increased the distance to open water, promoting a more continental climate not ameliorated by marine influences. Indeed, fossil insect evidence from eastern Chukotka suggests that the most important difference between LGM and recent climates in this region was increased continentality, i.e., a greatly enhanced amplitude between summer and winter temperatures (Alfimov and Berman, 2001). As the insect data of Alfimov and Berman (2001) suggest near present-day July temperatures for the region during MIS 2, the ~7°C lower mean annual temperatures derived from the Wrangel mammoth $\delta^{18}O$ data could be reached only by a significant lowering of the winter temperatures. This is consistent with the findings of $\delta^{18}O$ investigations of ground ice, representing winter precipitation, in Yakutia (Nikolaev and Mikhalev, 1995), generally showing depletions of 4-6‰, but reaching 8-10‰, relative to Holocene ice $\delta^{18}O$ values. The lower isotope values of MIS 2 correspond to mean January temperatures 10-14°C colder than at present (Nikolaev and Mikhalev, 1995). The Wrangel Island $\delta^{18}O$ interpretation highlights an important feature of the bioapatite $\delta^{18}O$ data discussed in this thesis. While providing quantitative information on the magnitude of $\delta^{18}O$ and temperature change between the glacial and interglacial periods, the bulk bioapatite samples do not offer clues into changes of seasonality. A lowering of the mean annual $\delta^{18}O$ value thus does not necessarily mean a balanced reduction of $\delta^{18}O$ values in winter and summer precipitation, but might be a result of, e.g., increased length of the cold period, or decreased $\delta^{18}O$ values in winter precipitation.

The palaeoenvironmental record in mammoth bioapatite ends at 4 ka, at a time of seemingly stable climatic conditions and range size. The bioapatite $\delta^{18}O$ data suggests that present-day climatic conditions were established in the area already at 10 ka with no significant fluctuations during the Holocene (Saarnisto and Karhu, 2004). This is consistent with the findings of Lozhkin et al. (2001) based on Wrangelian lacustrine deposits. Further, the $^{87}Sr/^{86}Sr$ record implies that the major palaeogeographical changes had already taken place by 10 ka. Thus, the isotopic signatures recorded in skeletal apatite provide valuable insight into the nature of the glacial and Holocene habitats of the mammoths, but the reason for their final demise remains unresolved.

4 Conclusion

The work presented here demonstrates the potential contained in the isotopic records of mammoth bioapatite for tackling diverse research problems related to past environments in the terrestrial realm. It contributes to the understanding of the latest ice age through new knowledge of the palaeoclimate and –ecology, and the effects of sea level rise. The research includes two new approaches: The Wrangel Island study demonstrates the use of bioapatite Sr isotope compositions in investigations of palaeogeographical isolation of animal populations and the underlying processes forcing the isolation. In isolation studies related to shoreline displacement, the Sr isotope approach has the advantage of not being dependent on bathymetry or the choice of eustatic sea level curve. The European mammoth enamel oxygen isotope record establishes the use of mammal $\delta^{18}O$ values for the reconstruction of continental-scale geographical $\delta^{18}O_{ppt}$ patterns. In addition, the bioapatite $\delta^{18}O$ record can also give insight into the minima and maxima associated with shorter time-scale climate fluctuations, not attainable from, e.g., palaeogroundwater archives.

The main palaeoenvironmental conclusions resulting from this thesis work can be summarised as follows:

- The $\delta^{18}O$ data obtained from the mammoth bioapatite indicate significant geographic variability in the magnitude of change in the $\delta^{18}O$ values and temperatures between the pre-LGM glacial climate and the present-day interglacial conditions. The long-term mean values of the oxygen isotope composition of precipitation in Europe at 52-24 ka were ~1-4‰ lower than those of the present-day precipitation. The regional differences can most likely be attributed to the persistence or absence of marine influence on the climate and changes in the palaeogeography during the glacial period.
- The temporal δ/T-slopes estimated on the basis of the palaeogroundwater data and present-day spatial gradients seem to give reasonable approximations of the glacial thermal climate in Europe, supporting previous assertions that in some regions the application of present-day spatial δ/T relationships to interpret past temperatures is warranted. The regional mean $\Delta^{18}O$ values, representing the total shift from the modern to the glacial $\delta^{18}O$ values, including the glacial ocean effect, imply 2-9°C lower annual surface temperatures in different regions.
- The reconstructed geographic distribution of the $\delta^{18}O_{ppt}$ values in glacial precipitation at 52-24 ka over Europe reflects a rainout pattern consistent with a large-scale atmospheric circulation resembling that of present-day, and westerly moisture sources for the entire area, including the areas most proximal to the Scandinavian Ice Sheet in northern Europe.
- The carbon isotope record in mammoth bioapatite is consistent with the climatic gradient inferred from the $\delta^{18}O$ values, and further implies differences in habitat openness in different parts of Europe. A temporal pattern of declining $\delta^{13}C$ values towards the end of the Pleistocene epoch, possibly related to the rise of atmospheric CO_2 levels, is detectable, but not as strong as that observed from other organic materials in Europe.
- The dramatic change in the global sea level is reflected in bioapatite $^{87}Sr/^{86}Sr$ ratios of the mammoth fauna in Wrangel Island, suggesting that the Holocene mammoths and the terminal Pleistocene animals had different foraging areas. The bioapatite Sr isotope ratios support earlier shoreline reconstructions indicating that the -40 m isobath was reached and the island isolated at ca. 10-10.5 ka. A shift toward more radiogenic bioapatite $^{87}Sr/^{86}Sr$ ratios after 8 ka is interpreted to reflect the rapid rise of the sea level from 10 to 8 ka, after which the mammoths were forced to inhabit less accessible regions of the island.

Acknowledgements

I wish to thank my supervisor Prof. Juha Karhu for introducing me to isotope geochemistry and making possible the research presented here. I have greatly benefited from his extensive knowledge in the field of isotope geoscience, and capability and readiness for scientific discourse that stems from this expertise. Over the course of the thesis work, I was given much space and independence to come up with my own solutions and hypotheses to be then critically disseminated in our discussions. More than anything, this has taught me the faculties required in scientific research.

I sincerely thank the official pre-examiners, Dr. Thomas Tütken and Dr. Kathryn Hoppe, for their thorough and constructive reviews and comments on the thesis.

For the funding of the thesis work I am grateful to the Finnish Academy of Science and Letters – Vilho, Yrjö and Kalle Väisälä Foundation, The Finnish Cultural Foundation and the Finnish Graduate School of Geology and its leader Prof. Veli-Pekka Salonen.

I thank my past and future co-authors and fellow mammoth researchers Kim Aaris-Sørensen, Linas Daugnora, Michael Houmark-Nielsen, Kurt Kjær, Lembi Lõugas, Piotr Wojtal and Ivars Zupins. Especially I wish to express my deepest gratitude to Pirkko Ukkonen, whose involvement, co-authorship, friendship and mentoring have in many ways shaped the thesis into its present form.

I am grateful to the Geological Survey of Finland, more specifically the people at the isotope laboratories – Hannu Huhma, Tuula Hokkanen, Arto Pulkkinen, Lasse Heikkinen, Arja Henttinen, Mia Tiljander and Nina Kortelainen – for collaboration and invaluable help with the isotope laboratory work.

All the people at the Department of Geology, University of Helsinki, are thanked for creating the friendliest and most supportive work environment imaginable. Particularly I offer my thanks to Liisa Nevalainen, Mia Kotilainen and Seija Kultti for the helpful discussions and empathy, and Tuija Vaahtojärvi for help in the laboratory.

On a more personal note I wish to thank my friends and family, who have been vital to my happiness and mental health, and whom I have severely neglected especially during the final year of thesis work. I am forever indebted to Joonas and Outi, who often faced the brunt of innumerable waves of despair, frustration and malaise, and provided constant encouragement, friendship, love and food.

References

Aaris-Sørensen, K., 2006. Northward expansion of the Central European megafauna during late Middle Weichselian interstadials, c. 45-20 kyr BP. Palaeontographia Abteilung A, 278, 125-133.

Aaris-Sørensen, K., Petersen., K.S., Tauber, H., 1990. Danish finds of mammoth (*Mammuthus primigenus* (Blumenbach)). Stratigraphical position and evidence of Late Pleistocene environment. Danmarks Geologiske Undersøgelse, Serie B 14, 1-44.

Alfano, M.J., Barron, E.J., Pollard, D., Huntley, B., Allen, J.R.M., 2003. Comparison of climate model results with European vegetation and permafrost during isotope stage three. Quaternary Research 59, 97-107.

Alfimov, A.V., Berman, D.I., 2001. Beringian climate during the Late Pleistocene and Holocene. Quaternary Science Reviews 20, 127-134.

Allen, J.R.M., Brandt, U., Brauer, A., Hubberten, H.-W., Huntley, B., Keller, J., Kram, M., Mackensen, A., Mingram, J., Negendank, J.F.W., Nowaczyk, N.R., Oberhänsli, H., Watts, W.A., Wulf, S., and Zolitschka, B., 1999. Rapid environmental changes in southern Europe during the last glacial period. Nature 400, 740-743.

Alley, R.B., 2000. The Younger Dryas cold interval as viewed from central Greenland. Quaternary Science Reviews 19, 213-226.

Alley, R.B., Cuffey, K.M., 2001. Oxygen- and hydrogen-isotopic ratios of water in precipitation: beyond paleothermometry. In: Valley, J.W., Cole, D.R. (eds), Stable isotope geochemistry. Reviews in Mineralogy and Geochemistry 43. Mineralogical Society of America, Washington, DC, pp. 527-550.

Ambrosiani, K.G., Robertsson, A.-M., 1992. Early Weichselian interstadial sediments at Härnösand, Sweden. Boreas 21, 305-317.

Andrews, J.N., Goldbrunner, J.E., Darling, W.G., Hooker, P.J., Wilson, G.B., Youngman, M.J., Eichinger, L., Rauert, W., Stichler, W., 1985. A radiochemical, hydrochemical and dissolved gas study of groundwaters in the Molasse Basin of Upper Austria. Earth and Planetary Science Letters 73, 317-332.

Arnold, N.S., van Andel, T.H., Valen, V., 2002. Extent and dynamics of the Scandinavian Ice Sheet during oxygen isotope stage 3 (65,000–25,000 yr BP). Quaternary Research 57, 38-48.

Ayliffe, L.K., Lister, A.M., Chivas, A.R., 1992. The preservation of glacial-interglacial climatic signatures in the oxygen isotopes of elephant skeletal phosphate. Palaeogeography, Palaeoclimatology, Palaeoecology 99, 179-191.

Ayliffe, L.K., Chivas, A.R., Leakey, M.G., 1994. The retention of primary isotope compositions of fossil elephant phosphate. Geochimica et Cosmochimica Acta 58, 5291-5298.

Bard, E., 1998. Geochemical and geophysical implications of the radiocarbon calibration. Geochimica et Cosmochimica Acta 62, 2025-2038.

Bar-Matthews, M., Ayalon, A., Kaufmann, A., 2000. Timing and hydrological conditions of sapropel events in the Eastern Mediterranean, as evidence from speleotems, Soreq Cave. Chemical Geology 169, 145-156.

Barron, E., Pollard, D., 2002. High-resolution climate simulations of oxygen isotope stage 3 in Europe. Quaternary Research 58, 296-309.

Beck, J.W., Richards, D.A., Edwards, R.L., Silverman, B.W., Smart, P.L., Donahue, D.J., Herrera-Osterheld, S., Burr, G.S., Calsoyas, L., Jull, A.J.T., Biddulph, D., 2001. Extremely large variations of atmospheric ^{14}C concentration during the last glacial period. Science 292, 2453-2458.

Bentaleb, I., Langlois, C., Martin, C., Iacumin, P., Carré, M., Antoine, P.-O., Duranthon, F., Moussa, I., Jaeger, J.-J., Barret, N., Kandrop, R., 2006. Rhinocerotid tooth enamel ^{18}O/^{16}O variability between 23 and 12 Ma in southwestern France. Comptes Rendus Geoscience 338, 172-179.

Bertleff, B., Ellwanger, D., Szenkler, C., Eichinger, L., Trimborn, P., Wolfendale, N., 1993. Interpretation of hydrodynamical and hydroisotopical measurements on palaeogroundwaters in Oberschwaben, South German Alpine foreland, with focus on Quaternary geology. In: Isotope techniques in the study of past and current environmental changes in the hydrosphere and the atmosphere. IAEA, Vienna, p. 337-357.

Beyerle, U., Putschert, R., Aeschbach-Hertig, W., Imboden, D.M., Loosli, H.H., Wieler, R., Kipfer, R., 1998. Climate and groundwater recharge during the last glaciation in an ice-covered region. Science 282, 731-734.

Birks, H.H., Ammann, B., 2000. Two terrestrial records of rapid climatic change during the glacial–Holocene transition (14,000–9,000 calendar years B.P.) from Europe. Proceedings of the National Academy of Sciences of the United States of America 97, 1390 -1394.

Björck, S., Walker, M.J.C., Cwynar, L.C., Johnsen, S., Knudsen, K.-L., Lowe, J.J., Wohlfarth, B., INTIMATE Members, 1998. An event stratigraphy for the Last Termination in the North Atlantic region based on the Greenland ice-core record: a proposal by the INTIMATE group. Journal of Quaternary Science 13, 283-292.

Blake, R.E., O'Neil, J.R., Garcia, G.A., 1997. Oxygen isotope systematics of biologically mediated reactions of phosphate: I. Microbial degradation of organophosphorous compounds. Geochimica et Cosmochimica Acta 61, 4411-4422.

Blum, J.D., Erel, Y., Brown, K., 1993. $^{87}Sr/^{86}Sr$ ratios of Sierra Nevada stream waters: implications for relative mineral weathering rates. Geochimica et Cosmochimica Acta 58, 5019-5025.

Bocherens, H., Mariotti, A., 1992. Biogéochimie isotopique du carbone dans les os de mammiferes actuels et fossiles de zones froides et tempérées. Comptes Rendus de l'Académie des Sciences de Paris 315, 1147-1153.

Bocherens, H., Fizet, M., Mariotti, A., Gangloff, R.R., Burns, J.A., 1994. Contribution of isotopic biogeochemistry (^{13}C, ^{15}N, ^{18}O) to the paleoecology of mammoths (*Mammuthus primigenius*). Historical Biology 7, 187-202.

Bocherens, H., Koch, P.L., Mariotti, A., Geraads, D., Jaeger, J.-J., 1996a. Isotopic biochemistry (^{13}C, ^{18}O) of mammal enamel from African Pleistocene hominid sites: implications for the preservation of paleoclimatic isotopic signals. Palaios 11, 397-408.

Bocherens, H., Pacaud, G., Lazarev, P.A., Mariotti, A., 1996b. Stable isotope abundances (^{13}C, ^{15}N) in collagen and soft tissues from Pleistocene mammals from Yakutia: Implications for the palaeobiology of the Mammoth Steppe. Palaeogeography, Palaeoclimatology, Palaeoecology 126, 31-44.

Bocherens, H., Billiou, D., Mariotti, A., Patou-Mathis, M., Otte, M., Bonjean, D. and Toussaint, M., 1999. Palaeonvironmental and palaeodietary implications of isotopic biogeochemistry of Last Interglacial Neanderthal and mammal bones in Scladina Cave (Belgium). Journal of Archaeological Science 26, 599-607.

Bos, J.A.A., Bohncke, S.J.P., Kasse, C., and Vandenberghe, J., 2001. Vegetation and climate during the Weichselian Early Glacial and Pleniglacial in the Niederlausitz, eastern Germany – macrofossil and pollen evidence. Journal of Quaternary Science 16, 269-289.

Bos, J.A.A., Helmens, K.F., Bohncke, S.J.P., Seppä, H., Birks, H.J.B., 2009. Flora, vegetation and climate at Sokli, northeastern Fennoscandia during the Weichselian Middle Pleniglacial. Boreas 38, 335-348.

Bowen, G.J., and Wilkinson, B., 2002. Spatial distribution of $\delta^{18}O$ in meteoric precipitation. Geology 30, 315-318.

Broecker, W.S., Peng, T.-H., Jouzel, J., Russell, G. 1990. The magnitude of global fresh-water transports of importance to ocean circulation. Climate Dynamics 4, 73-79.

Bryant, J.D., and Froelich, P.N., 1995. A model of oxygen isotope fractionation in body water of large mammals. Geochimica et Cosmochimica Acta 59, 4523-4537.

Bryant, J.D., Luz, B., Froelich, P.N., 1994. Oxygen isotope composition of fossil horse tooth phosphate as a record of continental paleoclimate. Palaeogeography, Palaeoclimatology, Palaeoecology 107, 303-316.

Bryant, J.D., Froelich, P.N., Showers, W.J., Genna, B.J., 1996a. Biologic and climatic signals in the oxygen isotopic composition of Eocene-Oligocene equid enamel phosphate. Palaeogeography, Palaeoclimatology, Palaeoecology 126, 75-89.

Bryant, J.D., Koch, P.L., Froelich, P.N., Showers, W.J., Genna, B.J., 1996b. Oxygen isotope partitioning between phosphate and carbonate in mammalian apatite. Geochimica et Cosmochimica Acta 60, 5145-5148.

Budd P., Montgomery J., Barreiro B., Thomas R.G., 2000. Differential diagenesis of strontium in archaeological human dental tissues. Applied Geochemistry 15, 687-694.

Burgman, J.O., Calles, B., Westman, F., 1987. Conclusions from a ten year study of oxygen-18 in precipitation and runoff in Sweden. Isotope Techniques in Water Resources Development, IAEA-SM-299/107, pp. 579-590.

Cerling. T.E., Harris, J.M., 1999. Carbon isotope fractionation between diet and bioapatite in ungulate mammals and implications for ecological and paleoecological studies. Oecologia 12, 347-363.

Cerling, T. E., Wang, Y.,Quade, J., 1993 Expansion of C4 ecosystems as an indicator of global ecological change in the late Miocene. Nature 361, 344-345.

Cerling, T.E., Harris, J.M., Leakey, M.G., 1999. Browsing and grazing in elephants the isotope record of modern and fossil proboscideans. Oecologia 120, 364-374.

Chadwick, O.A., Derry, L.A., Vitousek, P.M., Huebert, B.J., Hedin, L.O., 1999. Changing sources of nutrients during four million years of ecosystem development. Nature 397, 491-497.

Chamberlain, C.P., Blum, J.D., Holmes, R.T., Xiahong, Feng, Sherry, T.W., Graves, G.R., 1997. The use of isotope tracers for identifying populations of migratory birds. Oecologia 109, 132-141.

Chapman, M.R., Maslin, M.A., 1999. Low-latitude forcing of meridional temperature and salinity gradients in the subpolar North Atlantic and the growth of glacial ice sheets. Geology 27, 875-878.

Churcher, C.S., 1980. Did the North American mammoth migrate? Canadian Journal of Anthropology 1, 103-105.

Clementz, C.T., Koch, P.L., 2001. Differentiating aquatic mammal habitat and foraging ecology with stable isotopes in tooth enamel. Oecologia 129, 461-472.

Coope, G.R., 2002. Changes in the thermal climate in northwestern Europe during marine oxygen isotope stage 3, estimated from fossil insect assemblages. Quaternary Research 57, 401-408.

Craig, H., 1961. Isotopic variation in meteoric waters. Science 133, 1702-1703.

Cuffey, K.M., Alley, R.B., Stuiver, M., Waddington, E.D., Saltus, R.W., 1995. Large arctic temperature change at the Wisconsin-Holocene glacial transition. Science 270, 455-458.

Dansgaard, W., 1964. Stable isotopes in precipitation. Tellus 16, 436-468.

Darling, W.G., 2004. Hydrological factors in the interpretation of stable isotope data present and past: a European perspective. Quaternary Science Reviews 23, 743-770.

Darling, W.G., Edmunds, W.M., Smedley, P.L., 1997. The isotopic composition of palaeowaters in the British Isles. Applied Geochemistry 12, 813-829.

Darling, W.G., Bath, A.H., Talbot, J.C., 2003. The O and H stable isotopic composition of fresh waters in the British Isles. 2. Surface waters and groundwater. Hydrology and Earth System Sciences 7, 183-195.

Davydova, N., Servant-Vildary, S., 1996. Late Pleistocene and Holocene history of lakes in the Kola Peninsula, Karelia and the North-Western part of the East European plain. Quaternary Science Reviews 15, 997-1012.

DeNiro, M.J., Epstein, S., 1978. Influence of diet on the distribution of carbon isotopes in animals. Geochimica et Cosmochimica Acta 42, 495-506.

d'Obyrn, K., Grabczak, J., Zuber, A., 1997. Mapy skladów izotopowych infiltracji Holocenskiej na obszarza Polski. In: Gorski, J., Liszkowska, E. (eds), Wspolezesne problemy hydrogeologii. Tom VIII. Wind-J. Wojewoda, Wroclaw, pp. 331-333.

Dray, M., Ferhi, A., Jusserand, C., Olive, P., 1998. paleoclimatic indicators deduced from isotopic data in the main French deep aquifers. In: Isotope techniques in the study of environmental change. IAEA, Vienna, pp. 683-692.

Driessens, F.C.M., Verbeeck, R.M.H., 1990. Biominerals. CRC Press, Boca Raton, Florida.

Drucker, D., Bocherens, H., Bridault, A., Billiou, D., 2003. Carbon and nitrogen isotopic composition of red deer (*Cervus elaphus*) collagen as a tool for tracking palaeoenvironmental change during the Late-Glacial and Early Holocene in the northern Jura (France). Palaeogeography, Palaeoclimatology, Palaeoecology 195, 375-388.

Drucker, D.G., Bridault, A., Hobson, K.A., Szuma, E., Bocherens, H., 2008. Can carbon-13 in large herbivores reflect the canopy effect in temperate and boreal ecosystems? Evidence from modern and ancient ungulates. Palaeogeography, Palaeoclimatology, Palaeoecology 266, 69-82.

Edwards, T.D.W., Wolfe, B., MacDonald, G.M., 1996. Influence of changing atmospheric circulation on precipitation δ^{18}O-temperature relations in Canada during the Holocene. Quaternary Research 46, 211-218.

Elias, S.A., Short, S.K., Nelson, C.H., and Birks, H.H., 1996. Life and times of the Bering land bridge. Nature 382, 60-63.

Elliott, J.C., 2002. Calcium phosphate biominerals. In: Kohn, M.J., Rakovan, J., Hughes, J.M. (eds). Phosphates: Geochemical, geobiological, and materials importance. Reviews in Mineralogy and Geochemistry 48, 427. Mineralogical Society of America, Washington D.C., 742 pp.

Elorza, J., Astibia, H., Murelaga, X., Pereda-Superbiola, X., 1999. Francolite as a diagenetic mineral in dinosaur and other Upper Cretaceous reptile bones (Laño, Iberian Peninsula): microstructural, petrological and geochemical features. Cretaceous research 20, 169-187.

Engels, S., Bohncke, S.J.P., Bos, J.A.A., Brooks, S.J., Heiri, O., Helmens, K.F., 2008. Chironomid-based palaeotemperature estimates for notheast Finland during Oxygen Isotope Stage 3. Journal of Paleolimnology 40, 49-61.

Ericson, J.E., 1985. Strontium isotope characterization in the study of prehistoric human ecology. Journal of Human Evolution 14, 503-514.

Fairbanks, R.G., 1989. A 17,000-year glacio-eustatic sea level record: influence of glacial melting dates on the Younger Dryas event and deep ocean circulation. Nature 342, 637-642.

Fairbanks, R.G., Mortlock, A., Chiu, T-C., Cao, L., Kaplan, A., Guilderson, T.P., Fairbanks, T., Bloom, A., Grootes, P., and Nadeau, M-J., 2005. Radiocarbon calibration curve spanning 0 to 50,000 years BP based on paired ^{230}Th/^{234}U/^{238}U and ^{14}C dates on pristine corals. Quaternary Science Reviews 24, 1781-1796.

Feranec, R.S., 2004. Geographic variation in the diet of hypsodont herbivores from the Francholabrean of Florida. Palaeogeography, Palaeoclimatology, Palaeoecology 207, 359-369.

Fortelius, M., Eronen, J.T., Jernvall, J., Liu, L., Pushkina, D., Rinne, J., Tesakov, A., Vislobokova, I.A., Zhang, Z., Zhou, L. 2002. Fossil mammals resolve regional patterns of Eurasian climate change during 20 million years. Evolutionary Ecology Research 4, 1005-1016.

Fox, D.L., Fisher, D.C., Vartanyan, S., Tikhonov, A.N., Mol, D., Buigues, B., 2007. Paleoclimatic implications of oxygen isotopic variation in late Pleistocene and Holocene tusks of *Mammuthus primigenius* from northern Eurasia. Quaternary International 169-170, 154-165.

Fricke, H.C., O'Neil, J.R., 1999. The correlation between $^{18}O/^{16}O$ ratios of meteoric water and surface temperature: its use in investigating terrestrial climate change over geologic time. Earth and Planetary Science Letters 170, 181.196.

Fricke, H. C., O'Neil, J. R., Lynnerup, N., 1995. Oxygen isotope composition of human tooth enamel from medieval Greenland: linking climate and society. Geology 23, 869-872.

Furrer, H., Graf, H.R., Mäder, A., 2007. The mammoth site of Niederweningen, Switzerland. Quaternary International 164-165, 85-97.

Gadbury, C., Todd, L., Jahren, A.H., Amundson, R., 2000. Spatial and temporal variations in the isotopic composition of bison tooth enamel from the Early Holocene Hudson-Meng Bone Bed, Nebraska. Palaeogeography, Palaeoclimatology, Palaeoecology 157, 79-93.

Gaigalas, A., Serebryanny, L., Valueva, M., 1992. Middle Valdaian forest environments at Biržai, northern Lithuania. Boreas 21, 289-293.

Genoni, L., Iacumin, P., Nikolaev, V., Gribchenko, Yu., Longinelli, A., 1998. Oxygen isotope measurements of mammoth and reindeer skeletal remains: an archive of Late Pleistocene environmental conditions in Eurasian Arctic. Earth and Planetary Science Letters 160, 587-592.

Genty, D., Blamart, D., Ouahdi, R., Gilmour, M., Baker, A., Jouzel J., Van-Exter, S., 2003. Precise dating of Dansgaard-Oeschger climate oscillations in western Europe from stalagmite data. Nature 421, 833-837.

Gosz, J.R., Brookins, D.G., Moore, D.I., 1983. Using strontium isotope ratios to estimate inputs to ecosystems. BioScience 33, 23-30.

Graustein, W.C., 1989. $^{87}Sr/^{86}Sr$ ratios measure the sources and flow of strontium in terrestrial ecosystems. In: Stable isotopes in ecological research, Rundel PW, Ehleringer J.R., Nagy K.A. (eds). Springer-Verlag, New York, 491-512.

Graustein, W.C., Armstrong, R., 1983. The use of strontium-87/strontium-86 ratios to measure atmospheric transport into forested watersheds. Science 219, 289-292.

Grootes, P.M., Stuiver, M., Whilte, J.W.C., Johnsen, S., Jouzel, J., 1993. Comparison of oxygen isotope records from the GISP2 and GRIP Greenland ice cores. Nature 366, 552-554.

Guthrie, R.D., 1990. Frozen fauna of the mammoth steppe: the story of blue babe. The University of Chicago Press, Chicago, 338 pp.

Hammarlund, D., 1999. Ostracod stable isotope records from a deglacial isolation sequence in southern Sweden. Boreas 29, 564-574.

Hatté, C., Antoine, P., Fontugne, M., Rousseau, D.-D., Tisnérat-Laborde, N., Zöller, L., 1999. New chronology and organic matter $\delta^{13}C$ paleoclimatic significance of Nußloch loess sequence (Rhine Valley, Germany). Quaternary International 62, 85-91.

Haynes, G., 1991. Mammoths, Mastodons, and Elephants. Biology, Behavior and the Fossil Record. Cambridge University Press, Cambridge, 413 pp.

Heaton, T.H.E., 1999. Spatial, species, and temporal variations in the $^{13}C/^{12}C$ ratios of C3 plants: implications for palaeodiet studies. Journal of Archaeological Science 26, 637-649.

Hedges, R.E.M., Stevens, R.E., Richards, M.P., 2004. Bone as a stable isotope archive for local climatic information. Quaternary Science Reviews 23, 959-965.

Helmens, K.F., Bos, J.A.A., Engels, S., Van Meerbeeck, C.J., Bohncke, S.J.P., Renssen, H., Heiri, O., Brooks, S.J., Seppä, H., Birks, H.J.B., Wohlfarth, B., 2007. Present-day temperatures in northern Scandinavia during the last glaciation. Geology 35, 987-990.

Herz, O.V., 1902. Otchety nacha'lnuka ekspeditsii imperatorskoy akademii nauk na Beryozovku dlya raskopki trupa mamonta. Izvestiya Imperatorskoy Akademii Nauk 16, 137-174 (in Russian).

Hillson, S., 2005. Teeth. Cambridge Manuals in Archaeology. Second edition. Cambridge University Press, Cambridge, UK, pp. 146-148.

Hinsby, K., Harrar, W.G., Nyegaard, P., Konradi, P.B., Rasmussen, E.S., Bidstrup, T., Gregersen, U., Boaretto, E., 2001. The Ribe Formation in western Denmark – Holocene and Pleistocene groundwaters in a coastal Miocene sand aquifer. In: Edmunds, W.M., and Milne, C.J. (eds), Palaeowaters in coastal Europe: evolution of groundwater since the late Pleistocene. Geological Society, London, Special Publications 189. The Geological Society of London, London, pp. 29-48.

Hoppe, K.A., 1999. Correlation between the oxygen isotope ratio of North American bison teeth and local waters: implications for paleoclimatic reconstructions. Earth and Planetary Science Letters 244, 408-417.

Hoppe, K.A., Stuska, S., Amundson, R., 2005. The implications for paleodietary and paleoclimatic reconstructions of intrapopulation variability in the oxygen and carbon isotopes of teeth from modern and feral horses. Quaternary Research 64, 138-146.

Hoppe, K.A., Koch, P.L., 2006. The Biogeochemistry of the Aucilla river fauna. In: Webb, S.D. (ed), First Floridians and last mastodons: The Page-Ladson site in the Aucilla River. Topics in Geobiology vol. 26, p. 379-401. Springer, The Netherlands.

Hoppe K.A., Koch, P.L., Furutani, T.T, 2003. Assessing the preservation of biogenic strontium in fossil bones and tooth enamel. International Journal of Osteoarchaeology 13, 20-28.

Hoppe, K.A., 2004. Late Pleistocene mammoth herd structure, migration patterns, and Clovis hunting strategies inferred from isotopic analyses of multiple death assemblages. Paleobiology 30, 129-145.

Hoppe, K.A., Koch, P.L., 2007. Reconstructing the migration patterns of late Pleistocene mammals from northern Florida, USA. Quaternary Research 68, 347-352.

Hoppe, K., Koch, P.L., Carlson, R.W., Webb, S.D., 1999. Tracking mammoths and mastodons: reconstruction of migratory behavior using strontium isotope ratios. Geology 27, 439-442.

Houmark-Nielsen, M., 2004. The Pleistocene of Denmark: a review of stratigraphy and glaciation history. In: Ehlers, J., Gibbard, P. (eds), Quaternary Glaciations – Extent and Chronology Part I: Europe. Elsevier, Amsterdam, pp. 35-46.

Hughen, K., Southon, J., Lehman, S., Bertrand, C., Turnbull, J., 2006. Marine-derived ^{14}C calibration and activity record for the past 50,000 years updated from the Cariaco Basin. Quaternary Science Reviews 25, 3216-3227.

Huh, Y., Panteleyev, G., Babich, D., Zaitsev, A., and Edmond, J.M., 1998. The fluvial geochemistry of the rivers of Eastern Siberia: II. Tributaries of the Lena, Omoloy, Yana, Indigirka, Kolyma, and Anadyr draining the collisional/accretionary zone of the Verkhoyansk and Cherskiy ranges. Geochimica et Cosmochimica Acta 62, 2053-2075.

Huijzer, B., Vandenberghe, J., 1998. Climatic reconstruction of the Weichselian Pleniglacial in northwestern and central Europe. Journal of Quaternary Science 13, 391-417.

Huneau, F., Blavoux, B., Aeschbach-Hertig, W., Kipfer, R., 2002. Paleogroundwaters of the Valréas Miocene aquifer (southeastern France) as archives of the LGM/Holocene transition in the western Mediterranean region. In: Study of Environmental Change Using Isotope Techniques. Proceedings of an International Conference in Vienna, Austria, 23-27 April 2001. C&S Papers

Series No.13. IAEA, Vienna, pp. 84-90.

Huntley, B., Alfano, M.J., Allen, J.R.M., Pollard, D., Tzedakis, P., de Beaulieu, J.-L., Grüger, E., Watts, B., 2003. European vegetation during marine oxygen isotope stage-3. Quaternary Research 59, 195-212.

Iacumin, P., Bocherens, H., Mariotti, A., Longinelli, A., 1996a. Oxygen isotope analyses of co-existing carbonate and phosphate in biogenic apatite: a way to monitor diagenetic alteration of bone phosphate? Earth and Planetary Science Letters 142, 1-6.

Iacumin, P., Bocherens, H., Mariotti, A., Longinelli, A., 1996b. An isotopic palaeoenvironmental study of human skeletal remains from the Nile Valley. Palaeogeography, Palaeoclimatology, Palaeoecology 126, 15-30.

Iacumin, P., Nikolaev, V., Ramigni, M., 2000. C and N isotope measurements on Eurasian fossil mammals, 40 000 to 10 000 years BP: herbivore physiologies and palaeoenvironmental reconstruction. Palaeogeography, Palaeoclimatology, Palaeoecology 163, 33-47.

Iacumin, P., Bocherens, H., Delgado Huertas, A., Mariotti, A., Longinelli, A., 1997. A stable isotope study of fossil mammal remains from the Paglicci cave, Southern Italy. N and C as palaeoenvironmental indicatiors. Earth and Planetary Science Letters 148, 349-357.

Iacumin, P., Nikolaev, V., Ramigni, M., Longinelli, A., 2004. Oxygen isotope analyses of mammal bone remains from Holocene sites in European Russia: palaeoclimatic implications. Global and Planetary Change 40, 169-176.

IAEA/WMO, 2006. Global Network of Isotopes in Precipitation. The GNIP Database. Accessible at: http://isohis.iaea.org.

IAEA, 2006. Isotope Hydrology Information System. The ISOHIS Database. Accessible at: http://isohis.iaea.org

Johnsen, S., Clausen, H.B., Dansgaard, W., Fuhrer, K., Gundestrup, N., Hammer, C.U., Iversen, P., Jouzel, J., Stauffer, B., Steffensen, J.P., 1992. Irregular glacial interstadials recorded in a new Greenland ice core. Nature 359, 311-313.

Johnsen, S.J., Dahl-Jensen, D., Dansgaard, W. and Gundestrup, N.S., 1995. Greenland temperatures derived from GRIP bore temperature and ice core isotope profiles. Tellus B 47, 624-629.

Johnsen, S.J., Dahl-Jensen, D., Gundestrup, N., Steffensen, J.P., Clausen, H.B., Miller, H., Masson-Delmotte, V., Sveinbjörnsdottir, A.E., White, J., 2001. Oxygen isotope and palaeotemperature records from six Greenland ice-core stations: Camp Century, Dye-3, GRIP, GISP2, Renland and NorthGRIP. Journal of Quaternary Science 16, 299-307.

Johnsen, T., Alexanderson, H., Murray, A.S., 2008. Re-dating the Pilgrimstad interstadial: a warmer climate and a smaller ice sheet during the Swedish Middle Weichselian (MIS 3)? Conference abstract LED2008, Beijing, China, 18-22 September 2008.

Jones, A.M., O'Connell, T.C., Young, E.D., Scott, K., Buckingham, C.M., Iacumin, P., Brasier, M.D., 2001. Biogeochemical data from well preserved 200 ka collagen and skeletal remains. Earth and Planetary Science Letters 193, 143-149.

Jouzel, J., Alley, R.B., Cuffey, K.M., Dansgaard, W., Grootes, P., Hoffmann, G., Johnsen, J.S., Koster, R.D., Peel, D., Shuman, C.A., Stievenard, M., Stuiver, M., White, J., 1997. Validity of the temperature reconstruction from water isotopes in ice cores. Journal of Geophysical Research 102 (C12), 26471-26487.

Jouzel, J.. Hoffmann, G., Koster, R.D., Masson, V., 2000. Water isotopes in precipitation: data/model comparison for present-day and past climates. Quaternary Science Reviews 19, 363-379.

Karhu, J.A., Possnert, G., Saarnisto, M., and Vartanyan, S., 1998. Paleoclimatic change at the Pleistocene-Holocene boundary, Wrangel Island, eastern Siberia: evidence from oxygen isotopes in mammoth teeth. Eos Transactions, American Geophysical Union 79, F492.

Kasse, C., Huitzer, A.S., Krzyszkowski, D., Bohncke, S.J.P., Coope, G.R., 1998. Weichselian Late Pleniglacial and Late-glacial depositional environments, Coleoptera and perglacial climatic records from central Poland (Belchatów). Journal of Quaternary Science 13, 455-469.

Kitagawa, H., van der Plicht, J., 1998. Atmospheric radiocarbon calibration to 45,000 yr BP: Late Glacial fluctuations and cosmogenic isotope production. Science 279, 1187-1190.

Kitagawa, H., van der Plicht, J., 2000. Atmospheric radiocarbon calibration beyond 11,900 cal BP from Lake Suigetsu laminated sediments. Radiocarbon 42, 369-380.

Koch, P., Tuross, N., Fogel, M., 1997. The effects of sample treatment and diagenesis on the isotopic integrity of carbonate in biogenic hydroxylapatite. Journal of Archaeological Science 24, 417-429.

Koch, P.L., Halliday, A.N., Walter, L.M., Stearley, R.F., Huston, T.J., Smith, G.R., 1992. Sr isotopic composition of hydroxyapatite from recent and fossil salmon: the record of lifetime migration and diagenesis. Earth and Planetary Science Letters 108, 277-287.

Koch, P.L., Hoppe, K.A., Webb, S.D., 1998. The isotopic ecology of late Pleistocene mammals in North America Part 1. Florida. Chemical Geology 152, 119-138.

Kohn, M.J., Cerling, T.E., 2002. Stable isotope compositions of biological apatite. In: Kohn, M.J., Rakovan, J., Hughes, J.M. (eds). Phosphates: Geochemical, geobiological, and materials importance. Reviews in mineralogy & Geochemistry, vol. 48 Mineralogical Society of America, Washington D.C. p. 455-488.

Kohn, M.J., Schoeninger, M.J, Barker, W.W., 1999. Altered states: Effects of diagenesis on fossil tooth chemistry. Geochimica et Cosmochimica Acta 63, 2737-2747.

Kohn, M.J., 1996. Predicting animal $\delta^{18}O$: accounting for diet and physiological adaptation. Geochimica et Cosmochimca Acta 60, 4811-4829.

Kolodny, Y., Luz, B. Navon, O. 1983. Oxygen isotope variation in phosphate of biogenic apatites, I. Fish bone apatite – rechecking the rules of the game. Earth and Planetary Science Letters 64, 398-404.

Kortelainen, N.M., Karhu, J.A., 2004. Regional and seasonal trends in the oxygen and hydrogen isotope ratios of Finnish groundwaters: a key for mean annual precipitation. Journal of Hydrology 285, 143-157.

Kos'ko, M.K., Cecile, M.P., Harrison, J.C., Ganelin, V.G., Khandoshko, N.V., and Lopatin, B.G., 1993. Geology of Wrangel island, between Chukchi and East Siberian Seas, Northeastern Russia. Geological Survey of Canada Bulletin 461.

Krishnamurthy, R.V., Epstein, S., 1990. Glacial-interglacial excursion in the concentration of atmospheric CO_2: effect in the $^{13}C/^{12}C$ ratio in wood cellulose. Tellus B 42, 423-434.

Kurita, N., Yoshida, N., Inoue, G., Chayanove, E.A., 2004. Modern isotope climatology of Russia: a first assessment. Journal of Geophysical Research 109, D03102.

Lambeck, K., Yokoyama, Y., Purcell, T., 2002. Into and out of the Last Glacial Maximum: sea-level change during Oxygen Isotope Stages 3 and 2. Quaternary Science Reviews 21, 343-360.

Land, L.S., Lundelius, E.L. Jr, Valastro, S. Jr., 1980. Isotopic ecology of deer bones. Palaeogeography, Palaeoclimatology, Palaeoecology 32, 143-151.

Leavitt, S.W., Danzer, S.R., 1992. $\delta^{13}C$ variations in C3 plants over the past 50,000 years. Radiocarbon 34, 783-791.

Lécuyer, C., 2004. Oxygen isotope analysis of phosphate. In: de Groot, P. (ed.), Handbook of stable isotope analytical techniques, volume I. Elsevier, Amsterdam, pp. 482-496.

Lécuyer, C., Grandjean, P., Sheppard, S.M.F., 1999. Oxygen isotope exchange between dissolved phosphate and water in temperatures <135°C: Inorganic versus biological fractionations. Geochimica et Cosmochimica Acta 63, 855-862.

Le Gal La Salle, C., Marlin, C., Savoye, S., Fontes, J.C., 1996. Geochemistry and ^{14}C dating of groundwaters from Jurassic aquifers of the North Aquitane Basin (France). Applied Geochemistry 11, 433-445.

Lee-Thorp, J., 2000. Preservation of biogenic carbon isotopic signals in Plio-Pleistocene bone and tooth mineral. In: Ambrose, S.H., Katzenberg, M.A. (eds), Biogeochemical approaches to paleodietary analysis. Advances in Archaeological and Museum Science Volume 5. Kluwer Academic/Plenum Publishers, New York, p. 89-115.

Lee-Thorp, J., van der Merwe, N., 1991. Aspects of the chemistry of modern and fossil biological apatites. Journal of Archaeological Science 18, 343-354.

Lee-Thorp, J., Sponheimer, M., 2003. Three case studies used to reassess the reliability of fossil bone and enamel isotope signals for paleodietary studies. Journal of Anthropological Archaeology 22, 208-216.

Lee-Thorp, J.A. Sealy, J.C., van der Merwe, N.J., 1989. Stable carbon isotope ratio differences between bone and collagen and bone apatite, and their relationship to diet. Journal of Archaeological Science 16, 585-599.

Lister, A.M., Stuart, A.J., 2008. The impact of climate change on large mammal distribution and extinction: evidence from the last glacial/interglacial transition. Comptes Rendus Geosciences 340, 615-620.

Longinelli, A., 1984. Oxygen isotopes in mammal bone phosphate: a new tool for paleohydrological and paleoclimatological research? Geochimica et Cosmochimica Acta 48, 385-390.

Loosli, H.H., Aeschbach-Hertig, W., Barbecot, F., Blaser, P., Darling, W.G., Dever, L., Edmunds, W.M., Kipfer, R., Putschert, R., Walraevens, K., 2001. Isotopic methods and their hydrogeochemical context in the investigation of palaeowaters. In: Edmunds, W.M., and Milne, C.J. (eds), Palaeowaters in coastal Europe: evolution of groundwater since the late Pleistocene. Geological Society, London, Special Publications, 189. The Geological Society of London, London, 193-212.

Lõugas, L. Ukkonen, P., Jungner, H., 2002. Dating the extinction of European mammoths: new evidence from Estonia. Quaternary Science Reviews 21, 1347-1354.

Lozhkin, A.V., Anderson, P.M., Vartanyan, S.L., Brown, T.A., Belaya, B.V., and Kotov, A.N., 2001. Late Quaternary paleoenvironments and modern pollen data from Wrangel Island (Northern Chukotka). Quaternary Science Reviews 20, 217-233.

Luz, B., Kolodny, Y., 1985. Oxygen isotope variations in phosphate of biogenic apatites, IV. Mammal teeth and bones. Earth and Planetary Science Letters 75, 29-36

Luz, B., Kolodny, Y., Horowitz, M. 1984a. Fractionation of oxygen isotopes between mammalian bone-phosphate and environmental drinking water. Geochimica and Cosmochimica Acta 48, 1689-1693.

Luz, B., Kolodny, Y., Kovach, J., 1984b. Oxygen isotope variations in phosphate of biogenic apatites, III. Conodonts. Earth and Planetary Science Letters 69, 255-262.

Major, C.O., Goldstein, S.L., Ryan, W.B.F., Lericolais, G., Piotrowski, A.M., Hajdas, I., 2006. The co-evolution of Black Sea level and composition through the last deglaciation and its paleoclimatic significance. Quaternary Science Reviews 25, 2031-2047.

Manley, W.F., 2002. Postglacial flooding of the Bering land bridge: a geospatial animation. INSTAAR, University of Colorado, v1, [accessed 16 June 2008], http://instaar.colorado.edu/QGISL/bering_land_bridge.

Marino, B.D., McElroy, M.B., 1991. Isotopic composition of atmospheric CO_2 inferred from plant carbon in C4 plant cellulose. Nature 349, 127-131.

Marino, B.D., McElroy, M.B., Salawitch, R.J., Spaulding, W.G., 1992. Glacial-to-interglacial variations in the carbon isotopic composition of atmospheric CO^2. Nature 357, 461-466.

Markova, A., Simakova, A.N., Puzachenko, A.Yu., Kitaev, L.M., 2002. Environments of the Russian Plain during the Middle Valdai Briansk interstade (33,000-24,000 yr B.P.) indicated by fossil mammals and plants. Quaternary Research 57, 391-400.

Martin, C., Bentaleb, I., Kaandorp, R., Iacumin, P., Chatri, K., 2008. Intra-tooth study of modern rhinoceros enamel $\delta^{18}O$: is the difference between phosphate and carbonate $\delta^{18}O$ a sound diagenetic test? Palaeogeography, Palaeoclimatology, Palaeoecology 266, 183-189.

McArthur, J.M., Howarth, R.J., Bailey, T.R., 2001. Strontium isotope stratigraphy: LOWESS version 3: best fit to the marine Sr-isotope curve for 0-509 Ma and accompanying look-up table for deriving numerical age. The Journal of Geology 109, 155-170.

McCrea, J.M., 1950. On the isotopic chemistry of carbonates and a paleotemperature scale. The Journal of Chemical Physics 18, 849-857.

Mead, J.I., Agenbroad, L.D., Davis, O.K., Martin, P.S., 1986. Dung of *Mammuthus* in the arid southwest, North America. Quaternary Research 25, 121-127.

Miller, E.K., Blum, J.D., Friedland, A.J., 1993. Determination of soil exchangeable-cation loss and weathering rates using strontium isotopes. Nature 362, 438-441.

Moine, O., Rousseau, D.-D., Antoine, P., 2008. The impact of Dansgaard-Oeschger cycles on the loessic environment and malacofauna of Nussloch (Germany) during the Upper Weichselian. Quaternary Research 70, 91-104.

Molodkov, A., Bolikhovskaya, N., Miidel, A., Ploom, K., 2007. The sedimentary sequence recovered from the Voka outcrops, northeastern Estonia: implications for late Pleistocene stratigraphy. Estonian Journal of Earth Sciences 56, 47-62.

Moseley, K.A., 1982. Climatic changes in the Early Devensian cold stagge interpreted from Coleopteran assemblages. Unpublished PhD thesis, 259 pp. University of Birmingham.

Müller, W., Fricke, H., Halliday, A.N., McCulloch, M.T., Wartho, J.-A., 2003. Origin and migration of the Alpine iceman. Science 302, 862-866.

Nelson, B.K., DeNiro, M.J., Schoeninger, M.J., De Paolo, D.J., Hare, P.E., 1986. Effects of diagenesis on strontium, carbon nitrogen and oxygen concentrations and isotopic composition of bone. Geochimica et Cosmochimica Acta 50, 1941-1949.

Nikolaev, V., Mikhalev, D.V., 1995. An oxygen-isotope paleothermometer from ice in Siberian permafrost. Quaternary Research 43, 14-21.

O'Leary, M.H., 1988. Carbon isotopes in photosynthesis. Bioscience 38, 328-336.

O'Neil, J.R., Roe, L.J., Reinhard, E., Blake, R.E., 1994. A rapid and precise method of oxygen isotope analysis of biogenic phosphate. Israel Journal of Earth Sciences 43, 203-212.

Passey, B.H., Cerling, T.E., Levin, N.E., 2007. Temperature dependence of oxygen isotope acid fractionation for modern and fossil enamels. Rapid Communications in Mass Spectrometry 21, 2853-2859.

Peltier, W.R., 1994. Ice age paleotopography. Science 265, 195-201.

Petit, J.R., Jouzel, J., Raynaud, D., Barkov, N.I., Barnola, J.-M., Basile, I., Bender, M., Chapellaz, J., Davis, M., Delaygue, G., Delmotte, M., Kotlyakov, V.M., Legrand, M., Lipenkov, V.Y., Lorius, C., Pépin, L., Ritz, C., Saltzman, E., Stievenard, M., 1999. Climate and atmospheric history of the past 420,000 years from the Vostok ice core, Antarctica. Nature 399, 429-435.

Pollard, D., Barron, E., 2003. Causes of model-data discrepansies in European climate during oxygen isotope stage 3 with insights from the last glacial maximum. Quaternary Research 59, 108-113.

Poole, J., 1998. Report on noble gas analysis of fluids from Danish PALAEAUX water samples. The Noble Gas Hydrogeochemistry Laboratory, Postgraduate Research Institute for Sedimentology, Reading, UK.

Price, T.D., Gestsdóttir, H., 2006. The first settlers of Iceland: an isotopic approach to colonization. Antiquity 80, 130-144.

Price, T.D., Burton, J.H., Bentley, R.A., 2002. The Characterization of biologically available strontium isotope ratios for the study of prehistoric migration. Archaeometry 44, 117-135.

Punning, J.-M., Toots, M., Vaikmäe, R., 1987, Oxygen-18 in Estonian natural waters. Isotopenpraxis 28, 232-234.

Quade, J., Cerling, T.E., Barry, J.C., Morgan, M.E., Pilbeam, D.R., Chivas, A.R., Lee-Thorp, J.A., van der Merwe, N.J., 1992. A 16-Ma record of paleodiet using carbon and oxygen isotopes in fossil teeth from Pakistan. Chemical Geology. Isotope Geoscience Section 94, 183-192.

Reimer, P.J., Baillie, M.G.L., Bard, E., Bayliss, A., Beck, J.W., Bertrand, C.J.H., Blackwell, P.G., Buck, C.E., Burr, G.S., Cutler, K.B., Damon, P.E., Edwards, R.L., Fairbanks, R.G., Friedrich, M., Guilderson, T.P., Hogg, A.G., Hughen, K.A., Kromer, B., McCormac, F.G., Manning, S.W., Ramsey, C.B., Reimer, R.W., Remmele, S., Southon, J.R., Stuiver, M., Talamo, S., Taylor, F.W., van der Plicht, J., Weyhenmeyer, C.E., 2004, IntCal04 terrestrial radiocarbon age calibration, 26–0 ka BP. Radiocarbon 46, 1029-1058.

Remenda, V.H., Cherry, J.A., Edwards, T.W.D., 1994. Isotopic composition of old ground water from Lake Agassiz: implications for Late Pleistocene climate. Science 266, 1975-1978.

Renssen, H., Isarin, R.F.B., 2001. The two major warming phases of the last deglaciation at ~14.7 and ~11.5 ka cal BP in Europe: climate reconstructions and AGCM experiments. Global and Planetary Change 30, 117-153.

Richards, M.P., Hedges, R.E.M., 2003. Variations in $\delta^{13}C$ and $\delta^{15}N$ values of fauna from Northwest Europe over the last 40 000 years. Palaeogeography, Palaeoclimatology, Palaeoecology 193, 261-267.

Rinterknecht, V.R., Clark, P.U., Raisbeck, G.M., Yiou, F., Bitinas, A., Brook, E.J., Marks, L., Zelčs, V., Lunkka, J.-P., Pavlovskaya, I.E., Piotrowski, J.A., Raukas, A., 2006. The last deglaciation of the southeastern sector of the Scandinavian ice sheet. Science 311, 1449-1452.

Robertsson A-M., 1988. Biostratigraphical studies of interglacial and interstadial deposits in Sweden. Thesis, Department of Quaternary Research, University of Stockholm, Report 10.

Rozanski, K., Sonntag, C., Münnich, K.O., 1982. Factors controlling stable isotope composition of modern European precipitation. Tellus 34, 142-150.

Rozanski, K., 1985. Deuterium and oxygen-18 in European groundwaters – links to atmospheric circulation in the past. Chemical Geology (Isotope Geoscience Section) 52, 349-363.

Rozanski, K., Araguás-Araguás, L., and Gonfiantini, R., 1992. Relation between long-term trends of oxygen-18 isotope composition of precipitation and climate. Science 258, 981-985.

Rozanski, K., Araguás-Araguás, L., and Gonfiantini, R., 1993. Isotopic patterns in modern global precipitation. In: Swart, P.K., Lohmann, K.C., McKenzie, J., and Savin, S. (eds), Climate change in continental isotopic records. Geophysical Monograph 78, 1-37. American Geophysical Union.

Saarnisto, M., and Karhu, J., 2004. The last mammoths – palaeoenvironment of the Holocene mammoth on Wrangel Island. Quaternary Perspectives 14–1, 126-129.

Salonen, V.-P., Kaakinen, A., Kultti, S., Miettinen, A., Eskola, K.O., Lunkka, J.-P., 2008. Middle Weichselian glacial event in the central part of the Scandinavian Ice Sheet recorded in the Hitura pit, Ostrobothnia, Finland. Boreas 37, 38-54.

Satkūnas, J., Grigienė, A., Velichkevich, F., Robertsson, A.-M., and Sandgren, P., 2003. Upper Pleistocene stratigraphy at the Medininkai site, eastern Lithuania: a continuous record of the Eemian-Weichselian sequence. Boreas 32, 627-641.

Schoeninger, M.J., DeNiro, M.J., 1982. Carbon isotope ratios of apatite from fossil bone cannot be used to reconstruct diets of animals. Nature 297, 577-578.

Sealy, J.C., van der Merwe, N.J., Sillen, A., Kruger, F.J., Krueger, H.W., 1991. $^{87}Sr/^{86}Sr$ as a dietary indicator in modern and archaeological bone. Journal of Archaeological Science 18, 399-416.

Severinghaus, J.P., Sowers, T., Brook, E.J., Alley, R.B., Bender, M.L., 1998. Timing of abrupt climate change at the end of the Younger Dryas interval from thermally fractionated gases in polar ice. Nature 391, 141-146.

Sharp, Z.D., Atudorei, V., Furrer, H., 2000. The effect of diagenesis on oxygen isotope ratios of biogenic phosphates. American Journal of Science 300, 222-237.

Shemesh, A., Kolodny, Y., Luz, B., 1983. Oxygen isotope variation in phosphate of biogenic apatites, II. Phosphorite rocks. Earth and Planetary Science Letters 64, 405-416.

Shilo, N.A., Loshkin, A.V., Titov, E.E., Shumilov, Y.V., 1983. Kirgilyachskii mamont. Nauka: Moscow (in Russian).

Sillen, A., 1986. Biogenic and diagenetic Sr/Ca in Plio-Pleistocene fossils of the Omo Shungura Formation. Paleobiology 12, 311-323.

Sillen, A., Hall, G., Richardson, S., Armstrong, R., 1998. $^{87}Sr/^{86}Sr$ ratios in modern and fossil food-webs in the Starkfontein Valley: Implications for early hominid habitat preference. Geochimica et Cosmochimica Acta 62, 2463-2473.

Sponheimer, M., and Lee-Thorp, J.A., 2006. Enamel diagenesis at South Africal Australopith sites: implications for paleoecological reconstruction with trace elements. Geochimica et Cosmochimica Acta 70, 1644-1654.

Spötl, C., Mangini, A., 2002. Stalagmite from the Austrian Alps reveals Dansgaar-Oeschger events during isotope stage 3: implications for the absolute chronology of Greenland ice cores. Earth and Planetary Science Letters 203, 507-518.

Spötl, C., Vennemann, T.W. 2003. Continuous-flow isotope ratio mass spectrometric analysis of carbonate minerals. Rapid Communications in Mass Spectrometry 17, 1004-1006.

Spötl, C., Mangini, A., and Richards, D.A., 2006. Chronology and paleoenvironment of Marine Isotope Stage 3 from two high-elevation speleothems, Austrian Alps. Quaternary Science Reviews 25, 1127-1136.

Steffensen, J.P., Andersen, K.K., Bigler, M., Clausen, H.B., Dahl-Jensen, D., Fischer, H., Goto-Azuma, K., Hansson, M., Johnsen, S.J., Jouzel, J., Masson-Delmotte, V., Popp, T., Rasmussen, S.O., Röthlisberger, R., Ruth, U., Stauffer, B., Siggaard-Andersen, M.-L., Sveinbjörsdottir, Á.E., Svensson, A., White, J.W.C., 2008. High-resolution Greenland ice core data show abrupt climate change happens in few years. Science 321, 680-684.

Stephan, E., 2000. Oxygen isotope analysis of animal bone phosphate: method refinement, influence of consolidants, and reconstruction of palaeotemperatures for holocene sites. Journal of Archaeological Science 27, 523-535.

Stevens, R.E., Hedges, R.E.M., 2004. Carbon and nitrogen stable isotope analysis of northwest European horse bone and tooth collagen, 40,000 BP-present: palaeoclimatic interpretations. Quaternary Science Reviews 23, 977-991.

Stiévenard, M., Nikolaev, V., Bol'shiyanov, D., Fléhoc, C., Jouzel, J., Klementyev, O., Souchez, R., 1996. Pleistocene ice at the bottom of the Vavilov ice cap Severnaya Zemlya, Russian Arctic. Journal of Glaciology 42, 403-406.

Stuart, A.J., Lister, A.M., 2001. The mammalian faunas of Pakefield/Kessingland and Corton, Suffolk, UK: evidence for a new temperate episode in the British early Middle Pleistocene. Quaternary Science Reviews 20, 1677-1692.

Stuart, A.J., Sulerzhitsky, L.D., Orlova, L.A., Kuzmin, Y.V., Lister, A.M., 2002. The latest woolly mammoths (*Mammuthus primigenius* Blumenbach) in Europe and Asia: a review of evidence. Quaternary Science Reviews 21, 1559-1569.

Stuiver, M., Braziunas, T.F., 1987. Tree cellulose $^{13}C/^{12}C$ isotope ratios and climatic change. Nature 328, 58-60.

Stuiver, M., Reimer, P.J., and Reimer, R.W., 2005, CALIB 5.0. [WWW program and documentation]. http://radiocarbon.pa.qub.ac.uk/calib/, [accessed 20 June 2008].

Stute, M., Deák, J., 1989. Environmental isotope study (^{14}C, ^{13}C, ^{18}O, D, noble gases) on deep groundwater circulation systems in Hungary with reference to paleoclimate. Radiocarbon 31, 902-918.

Sullivan, C.H., Krueger, H.W., 1981. Carbon isotope analysis of separate chemical phases in modern and fossil bone. Nature 292, 333-335.

Sun, J., 2005. Nd and Sr isotopic variations in Chinese eolian deposits during the past 8 Ma: implications for provenance change. Earth and Planetary Science Letters 240, 454-466.

Svensson, A., Biscaye, P.E., and Grousset, F., 2000. Characterization of late glacial continental dust in the Greenland Ice Core Project ice core. Journal of Geophysical Research 105, 4637-4656.

Swart, P.K., Burns, S., Leder, J., 1991. Fractionation of the stable isotopes of oxygen and carbon in carbon dioxide during the reaction of calcite with phosphoric acid as a function of temperature and technique. Chemical Geology 86, 89-96.

Tanaka, T.Y., Chiba, M., 2006. A numerical study of the contributions of dust source regions to the global dust budget. Global and Planetary Change 52, 88-104.

Tudge, A.P., 1960. A method of analysis of oxygen isotopes in orthophosphate – its use in the measurement of paleotemperatures. Geochimica et Cosmochimica Acta 18, 81-93.

Tütken, T., Vennemann, T.W., Janz, H., Heizmann, E.P.J., 2006. Palaeoenvironment and palaeoclimate of the Middle Miocene lake in the Steinheim basin, SW Germany: a reconstruction from C, O, and Sr isotopes of fossil remains. Palaeogeography, Palaeoclimatology, Palaeoecology 241, 457-491.

Tütken, T., Furrer, H., Vennemann, T.W., 2007. Stable isotope compositions of mammoth teeth from Niederweningen, Switzerland: implications for the Late Pleistocene climate, environment and diet. Quaternary International 164–165, 139-150.

Tütken, T., Vennemann, T.W., Pfretzschner, H.-U., 2008. Early diagenesis of bone and tooth apatite in fluvial and marine settings: constraints from combined oxygen isotope, nitrogen and REE analysis. Palaeogeography, Palaeoclimatology, Palaeoecology 266, 254-268.

Ukkonen, P., Lunkka, J. P., Jungner, H., Donner, J., 1999. New radiocarbon dates from Finnish mammoths indicating large ice-free areas in Fennoscandia during the Middle Weichselian. Journal of Quaternary Science 14/7, 711-714.

Ukkonen, P., Arppe, L., Houmark-Nielsen, M., Kjaer, K.H., Karhu, J.A., 2007. MIS 3 mammoth remains from Sweden—implications for faunal history, palaeoclimate and glaciation chronology. Quaternary Science Reviews 26, 3081-3098.

Ukkonen, P., Aaris-Sørensen, K., Arppe, L., Clark, P.U., Daugnora, L., Lister, A. Lõugas, L., Seppä, H.A., Stuart, T., Wojtal, P., Zupins, I. Northern Europe in the Middle to Late Weichselian: the mammoth perspective. In preparation.

Ukraintseva, V.V., 1986. On the composition of the forage of large herbivorous mammals of the mammoth epoch: significance for palaeobiological and palaeogeographical reconstruction. Quartärpaläontologie 6, 231-238.

van Andel, T., 2002. The climate and landscape of the middle part of the Weichselian glaciation in Europe: the stage 3 project. Quaternary Research 57, 2-8.

van Andel, T.H., Tzedakis, P.C., 1996. Palaeolithic landscapes of Europe and environs 150,000-25,000 years ago: an overview. Quaternary Science Reviews 15, 481-500.

van der Merwe, N.J., Medina, E., 1989. Photosynthesis and $^{13}C/^{12}C$ ratios in Amazonian rain forests. Geochimica et Cosmochimica Acta 53, 1091-1094.

van der Merwe, N.J., Medina, E., 1991. The canopy effect, carbon isotope ratios and foodwebs in Amazonia. Journal of Archaeological Science 18, 249-259.

van der Merwe, N.J., Lee-Thorp, J.A., Thackerey, J.F., Hall-Martin, A., Kruger, F.J., Coetzee, H., Bell, R.H.V., Lindeque, M., 1990. Source-area determination of elephant ivory by isotopic analysis. Nature 346, 744-746.

van der Plicht, J., Beck, J.W., Bard, E., Baillie, M.G.L., Blackwell, P.G., Buck, C.E., Friedrich. M. Guilderson, T.P., Hughen, K.A., Kromer, B., McCormac, Fl.G., Bronk Ramsey, C., Reimer, P.J., Reimer, R.W., Remmele, S., Richards, D.A., Southon, J.R., Stuiver, M., Weyhenmeyer, C.E., 2004. NotCal04 – Comparison / Calibration ^{14}C records 26-50 cal kBP. Radiocarbon 46, 1225-1238.

van Geel, B., Aproot, A., Baittinger, C., Birks, H.H., Bull, I.D., Cross, H.B., Evershed, R.P., Gravendeel, B., Kompanje, E.J.O., Kuperus, P., Mol, D., Nierop, K.G.J., Pals, J.P., Tikhonov, A., van Reenen, G., van Tienderen, P.H., 2008. The ecological implications of a Yakutian mammoth's last meal. Quaternary Research 69, 361-376.

van Huissteden, K., Vandenberghe, J., Pollard, D., 2003. Palaeotemperature reconstructions of the European permafrost zone during marine oxygen isotope Stage 3 compared with climate model results. Journal of Quaternary Science 18, 453-464.

van Klinken, G.J., Richards, M.P., Hedges, R.E.M., 2000. An overview of causes for stable isotopic variations in past European human populations: environmental, ecophysiological, and cultural effects. In: Ambrose, S.H., Katzenberg, M.A. (eds), Biogechemical approaches to paleodietary analysis. Advances in Archaeological and Museum Science, vol. 5. Kluwer Academic/Plenum Publishers, New York, p. 39-63.

van Klinken, G.J., van der Plicht, J., Hedges, R.E.M., 1994. Bone $^{13}C/^{12}C$ ratios reflect (paleo-)climatic variations. Geophysical Research Letters 21, 445-448.

van Meerbeeck, C.J., Renssen, H., Roche, D.M., 2009. How did Marine Isotope Stage 3 and Last Glacial Maximum climates differ? – Perspectives from equilibrium simulations. Climates of the Past 5, 33-51.

Vartanyan, S.L., Garutt, V.E., Sher, A.V., 1993. Holocene dwarf mammoths from Wrangel Island in the Siberian Arctic. Nature 362, 337-340.

Vartanyan, S.L., Arslanov, Kh.A., Tertychnaya, T.V., Chernov, S.B., 1995. Radiocarbon dating evidence for mammoths on Wrangel Island, Arctic Ocean, until 2000 BC. Radiocarbon 37, 1-6.

Vartanyan, S.L., Arslanov, K.A., Karhu, J.A., Possnert, G., Sulerzhitsky, L.D., 2008. Collection of radiocarbon dates on the mammoths (*Mammuthus primigenius*) and other genera of Wrangel Island, northeast Siberia, Russia. Quaternary Research 70, 51-59.

Väliranta, M., Kultti, S., Seppä, H., 2006. Vegetation dynamics during the Younger Dryas-Holocene transition in the extreme northern taiga zone, northeastern European Russia. Boreas 35, 202-212.

Vedin, H., 2007. Jämtlands klimat. Väder och Vatten 1/2007, 10-11. SMHI.

Velichko, A.A., Zelikson, E.M., 2005. Landscape, climate and mammoth food resources in the East European Plain during the Late Paleolithic epoch. Quaternary International 126-128, 137-151.

Vennemann, T.W., Fricke, H.C., Blake, R.E., O'Neil, J.R., Colman, A., 2002. Oxygen isotope analysis of phosphates: a comparison of techniques for analysis of Ag_3PO_4. Chemical Geology 185, 321-336.

Vereshchagin, N.K., Baryshnikov, G.F., 1982. Paleoecology of the mammoth fauna in Eurasian arctic. In: Hopkins, D.M., Matthews, Jr., J.V., Schweger, C.E., Young, S.B. (eds), Paleoecology of Beringia. Academic Press, New York, p. 267-279.

Viscosi-Shirley, C., Mammone, K., Pisias, N., and Dymond, J., 2003. Clay mineralogy and multi-element chemistry of surface sediments on the Siberian-Arctic shelf: implications for sediment provenance and grain size sorting. Continental Shelf Research 23, 1175-1200.

Voelker, A.H.L., Sarnthein, M., Grootes, P.M., Erlenkeuser, H., Laj, C., Mazaud, A., Nadeau, M.-J., Schleicher, M., 1998. Correlation of marine ^{14}C ages from the Nordic Seas with the GISP2 isotope record: implications for ^{14}C calibration beyond 25 ka BP.

Voelker, A.H.L., workshop participants, 2002. Global distribution of centennial-scale records for Marine Isotope Stage (MIS) 3: a database. Quaternary Science Reviews 21, 1185-1212.

Vogel, J.C., Eglington, B., Auret, J.M., 1990. Isotope fingerprints in elephant bone and ivory. Nature 346, 747-749.

von Grafenstein, U., Erlenkeuser, H., Brauer, A., Jouzel, J., Johnsen, S.S., 1999. A mid-European decadal isotope-climate record from 15 500 to 5000 years BP. Science 284, 1654-1657.

Wang, Y., Cerling, T.E., 1994. A model for fossil tooth and bone diagenesis: implications for paleodiet reconstruction from stable isotopes. Palaeogeography, Palaeoclimatology, Palaeoecology 107, 281-289.

Weninger, B., Jöris, O., 2008. A ^{14}C age calibration curve for the last 60 ka: the Greenland-Hulu U/Th timescale and its impact on understanding the Middle to Upper Paleolithic transition in Western Eurasia. Journal of Human Evolution 55, 772-781.

Weninger, B., Jöris, O., Danzeglocke, U., 2008. CalPal-2007. Cologne Radiocarbon Calibration & Palaeoclimate Research Package. http://www.calpal.de/, [accessed 18.9.2008].

Weninger, B., Danzeglocke, U., Jöris, O., 2007. Comparison of dating results achieved using different radiocarbon-age calibration curves and data. http://www.calpal.de/calpal/files/CalCurveComparisons.pdf, [accessed 16.6.2009].

Williams, R.A.D., Elliott, J.C., 1989. Basic and applied dental biochemistry. Dental series. Churchill Livingstone, Edinburgh.

Wohlfarth, B., Lacourse, T., Bennike, O., Subetto, D., Tarasov, P., Demidov, I., Filimonova, L., Sapelko, T., 2007. Climatic and environmental changes in north-western Russia between 15,000 and 8000 cal yr BP: a review. Quaternary Science Reviews 26, 1871-1883.

Wojtal, P., Sobczyk, K., 2005. Man and woolly mammoth at the Kraków Spadzista Street (B) – taphonomy of the site. Journal of Archaeological Science 32, 193-206.

Wysota, W., Lankauf, K. R., Szmanda, J., Chruscinska, A., Oczkowski, H. L., Przegietka, K. R., 2002. Chronology of the Vistulian (Weichselian) glacial events in the Lower Vistula Region, Middle-North Poland. Geochronometria 21, 137-142.

Yokoo, Y., Nakano, T., Nishikawa, M., Quan, H., 2004. Mineralogical variation of Sr-Nd isotopic and elemental compositions in loess and desert sand from the central Loess Plateau in China as a provenance tracer of wet and dry deposition in the northwestern Pacific. Chemical Geology 204, 45-62.

Zazzo, A., Lécuyer, C., Mariotti, A., 2004a. Experimentally-controlled carbon and oxygen isotope exchange between bioapatites and water under inorganic and microbially-mediated conditions. Geochimica et Cosmochimica Acta 68, 1-12.

Zazzo, A., Lécuyer, C., Sheppard, S.M.F., Grandjean, P., Mariotti, A., 2004b. Diagenesis and reconstruction of paleoenvironments: a method to restore original δ^{18}O values of carbonate and phosphate from fossil tooth enamel. Geochimica et Cosmochimica Acta 68, 2245-2258.

Zazzo, A., Patterson, W.P., Prokopiuk, T.C., 2009. Comment on “Implications of digenesis for the isotopic analysis of upper Miocene large mammalian herbivore tooth enamel from Chad” by L. Jacues, N. Ogle, I. Moussa, R. Kalin, P. Vignaud, M. Brunet, and H. Bocherens [Palaeogeography, Palaeoclimatology, Palaeoecology 266 (2008) 200-210]. Palaeogeography, Palaeoclimatology, Palaeoecology 277, 265-268.

Zuber, A., Weise, S.M., Motyka, J., Osenbrück, K., Różański, K., 2004. Age and flow pattern of groundwater in a Jurassic limestone aquifer and related Tertiary sands derived from combined isotope, noble gas and chemical data. Journal of Hydrology 286, 87-112.

Zuzevičius, A., Mažeika, J., Baltrūnas, V., 2007. A model of brackish groundwater formation in the Nemunas River valley, Lithuania. Geologija 60, 63-75.